

RESEARCH MEMORANDUM

STABILITY OF SUPERSONIC INLETS AT MACH 1.91

WITH AIR INJECTION AND SUCTION

By K. Kowalski and Thomas G. Piercy

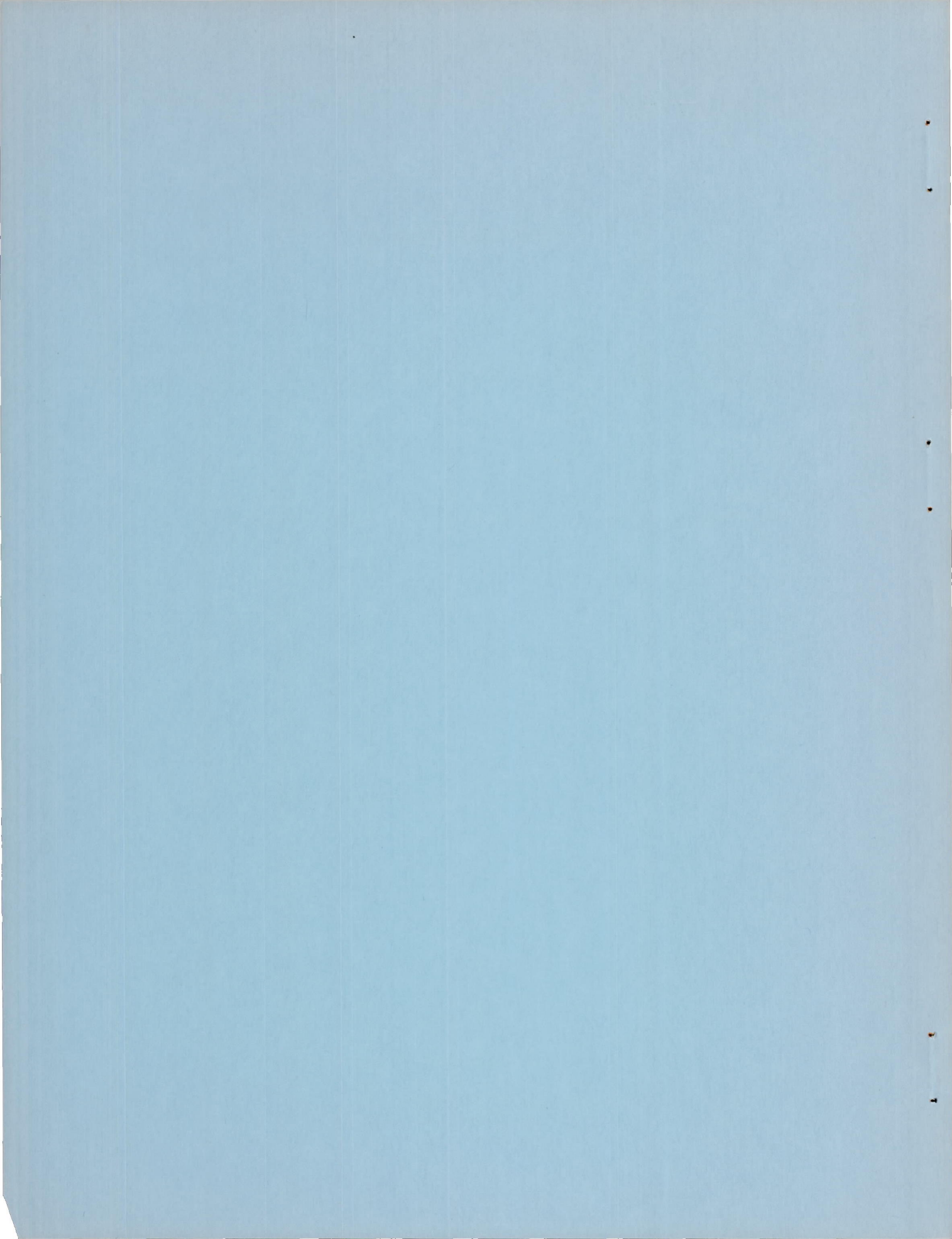
Lewis Flight Propulsion Laboratory
Cleveland, Ohio

NATIONAL ADVISORY COMMITTEE
FOR AERONAUTICS

WASHINGTON

June 28, 1956

Declassified July 22, 1959



NATIONAL ADVISORY COMMITTEE FOR AERONAUTICS

RESEARCH MEMORANDUM

STABILITY OF SUPERSONIC INLETS AT MACH 1.91

WITH AIR INJECTION AND SUCTION

By K. Kowalski and Thomas G. Piercy

SUMMARY

The stability characteristics of an axisymmetric conical inlet with supercritical spillage were investigated. The inlet cone was modified to incorporate a rearward-facing slot through which air could be bled or injected. The effects of cowl perforations were also investigated.

Either injection or suction through the slot increased the stable subcritical range over that of the unmodified cone as much as 22 percent of the free-stream mass flow. Only small decreases in pressure recovery were associated with these gains. The configurations using suction were more stable at angle of attack than those for which air was injected. In both cases, stable entry of the vortex sheet was observed.

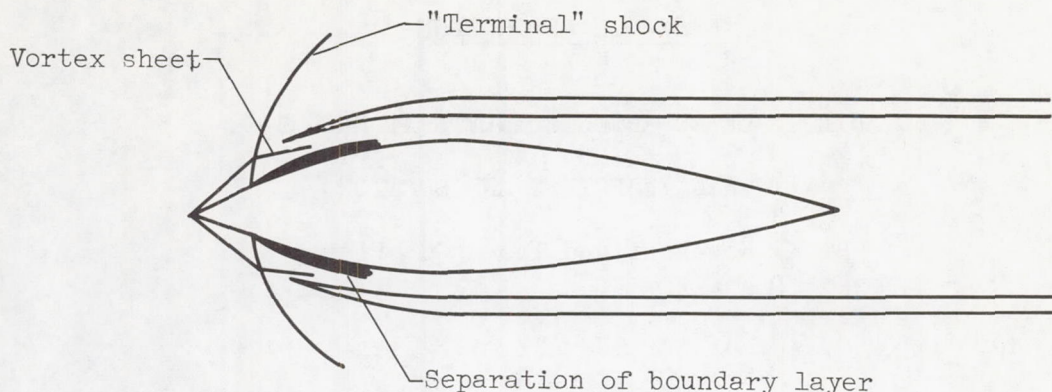
Cowl perforations were also effective in increasing the stable subcritical range. Increases of up to 11 percent of the free-stream mass flow over that of the unmodified inlet were obtained. No instability was observed when the vortex sheet entered the inlet. Simultaneous use of cowl perforations and injection proved no more effective in stabilizing the inlet than injection alone.

Stable entrance of the vortex sheet was also obtained by using the inlet modified by tip roughness or a wire boundary-layer trip. However, the increases in the stable range were at most 6 percent of free-stream mass flow, compared with the unmodified cone, and in most cases less than this value.

INTRODUCTION

To date, many investigations have been made concerning the subcritical instability which occurs in supersonic diffusers (refs. 1 to 3). Two phenomena which have been associated with the initiation of this instability in external-compression diffusers are (1) the separation of the centerbody boundary layer by the inlet terminal shock and (2) the

entrance of the vortex sheet arising from the oblique-terminal-shock intersection (see sketch).



The instability which may arise in conjunction with the first phenomenon is explained by the abrupt choking effect produced by the separation (refs. 1 and 2). This choking is followed by a forward shock movement, flow spillage, a subsequent reattachment of flow, and an aft shock movement. Then the cycle is repeated. The pressure rise across the terminal shock is the factor influencing this type of separation (ref. 4).

The second phenomenon was first related to the onset of instability in reference 2. For Mach numbers greater than about 1.7, the entry of the vortex sheet is nearly always associated with some amount of instability (refs. 1 to 3 and 5). It has been suggested that this entry may also result in the abrupt choking of the inlet flow. Then the cycle is similar to that previously described.

Both of the preceding phenomena associated with subcritical instability are similar. They both involve low-energy flows which subsequently separate or in any case choke the inlet flow. Two methods immediately evident for alleviating these effects are the removal or energizing of this low-energy flow. The flow may be removed by suction on the external-compression (refs. 3 and 6) and inner-cowl surfaces. In order to attain an energizing effect, air may be injected on the external-compression surface (ref. 7) or induced-mixing devices may be used (ref. 3).

The present study is part of a general investigation of subcritical instability which is being conducted at the NACA Lewis laboratory. The first purpose of this phase of the investigation was to determine whether the instability associated with the vortex-sheet entry could be alleviated by compression-surface boundary-layer control. The second purpose was to examine the effect on stability of directly removing low-energy air

resulting from the terminal shock by use of cowl perforations. The tests were conducted at Mach 1.91 with a single-shock conical inlet.

SYMBOLS

The following symbols are used in this report:

A	flow area, sq ft
m	mass flow, ρuA , slugs/sec
P	average total pressure, lb/sq ft
ΔP	maximum decrement in total pressure, as obtained from rake measurements, lb/sq ft
$\Delta P/P$	distortion parameter
p	static pressure, lb/sq ft
R	radius of spike tip at slot (fig. 1(b)), ft
S	slot height, ft
S/R	slot parameter
u	flow velocity, ft/sec
x	axial distance along diffuser, measured from inlet face, in.
α	angle of attack, deg
ρ	density, slugs/cu ft

Subscripts:

av	average
cr	conditions at inlet critical point
min	conditions at inlet minimum stable point
t	conditions at diffuser throat
O	free stream
l	secondary-flow condition

2 diffuser station, at rake

APPARATUS AND PROCEDURE

The investigation was conducted in the 18- by 18-inch Mach 1.91 tunnel at the NACA Lewis laboratory. The test conditions were a pressure altitude of 48,000 feet, a total temperature of 150° F, and a Reynolds number per foot of 3.2×10^6 . The dew point varied from -24° to -2°.

The inlet utilized in these tests was a modification of the inlet reported in reference 5 and was an all-external-compression axisymmetric design with a conical centerbody of 25° semivertex angle (fig. 1(a)). The cowl was positioned to have supercritical spillage, a configuration which is known to become unstable upon entry of the vortex sheet (ref. 5). The external cone surface was modified to incorporate a rearward-facing secondary-flow slot similar to that of reference 7. The slot height S (fig. 1(b)) was varied by translating the spike tip with respect to the centerbody and cowl. When the slot was closed, the configuration was designed to allow approximately 4-percent supercritical spillage. As the tip was translated forward, the amount of spillage increased. The slot was used either to inject high-energy air or to bleed off the compression-surface boundary layer. For injection, the high-pressure source was the atmosphere. In the case of suction the air was dumped into the test section after passing out of the model and through a rotameter. Further detail on the ducting may be seen from figure 1 along with the subsonic-diffuser-area variation and the model instrumentation.

For some configurations the cowl was perforated with two circumferential rows of ninety 1/16-inch-diameter holes. The first row was located 1/8 inch from the cowl lip; the second row was 1/4 inch from the lip. Tests were made with each row individually and in combination.

The average diffuser total pressure was computed by area-weighting the rake pitot-tube readings. Inlet mass flow was computed from the diffuser static pressure and an outlet-plug flow calibration. To compute the injection and bleed mass flows, a calibrated rotameter was used.

The occurrence of instability was determined visually. The minimum stable point was defined as that point which immediately preceded any shock oscillation. In the course of the investigation, a pressure cell was used to record the onset and magnitude of the oscillations. It was found that the readings of the cell, indicating the onset of unsteady flow, coincided with the observations of terminal-shock oscillation.

RESULTS AND DISCUSSION

Effect of Spike Tip Translation on Inlet Performance

In order to better understand the effect of injection or suction on the cone surface, it is necessary to examine first the departure from the unmodified-cone performance (ref. 5) which resulted from the surface discontinuity and translation of the tip alone (no secondary flow). The extent of the discontinuity and translation of the tip are related by the slot parameter S/R .

It is important to note that for S/R of 0 (slot fully closed) there was still a small discontinuity in the cone surface. This was a result of the effort to achieve the most effective angle of injection. Therefore, for all values of S/R (both with and without secondary flow) two oblique shocks were generated. The second (weaker) shock was formed after the flow expanded around the small step made by the slot.

The inlet pressure-recovery mass-flow characteristics for various values of S/R are presented in figure 2. The maximum inlet mass flow decreased as S/R increased. This was to be expected since the tip was translated with the relative position of the cowl and centerbody held constant. For S/R of 0, the total-pressure recovery was improved over that of the unmodified cone. This increase may have been due to the influence of the second shock. However, the recovery fell off quite rapidly with increasing S/R . The stability was improved slightly at 0° and 3° angles of attack for S/R of 0 over that of the unmodified cone. However, the stability decreased for increasing S/R . This reduced stability may have been due to the separation induced by the step. For large values of S/R , some configurations became unstable even before the vortex sheet entered.

Effect of Air Injection and Suction

The total-pressure mass-flow characteristics of the inlets are presented in figures 3, 4, 5, and 6 for the cases of injection, suction, cowl perforations, and injection plus cowl perforations, respectively. For comparison, the performance of the unmodified cone (ref. 5) and the performance of the modified cone at S/R of 0 are also shown. Discussion of the effects of these modifications, however, is based on summary curves which present the variations in critical and minimum stable mass flows and peak total-pressure recovery (fig. 7). The stable subcritical range shall be defined as the difference between the critical and minimum stable mass-flow ratios.

With injection, the maximum range of subcritical stability was obtained at a value of S/R of 0.113 for 0° and 3° angles of attack and

0.0565 for a 6° angle of attack (fig. 7(a)). For these values of S/R at 0° , 3° , and 6° angles of attack, the increases in the stable subcritical range over that of the unmodified cone were 23.5, 12.5, and 8.5 percent, respectively, of the free-stream mass flow. With the exception of S/R of 0.471, the critical mass flow remained nearly constant as S/R was changed. The peak pressure recovery, however, decreased continually as S/R was increased. At the gap width corresponding to maximum stable subcritical operation (S/R , 0.113), the peak recovery was decreased about 2.5 percent below that for S/R of 0.

With suction, the maximum stable subcritical range occurred at S/R of 0.169 at 0° and 3° angles of attack and at S/R of 0.225 at a 6° angle of attack (fig. 7(b)). For these values of S/R at 0° , 3° , and 6° angles of attack, the increases in the stable subcritical range, as compared with the unmodified cone, were 22, 22, and 17.5 percent of the free-stream mass flow. For some values of S/R , there were some regions of small amplitude instability when the terminal shock was near the bleed slot (fig. (4)). The inlet became stable again when the terminal shock was positioned upstream of the slot. However, the minimum stable mass flow referred to in the preceding calculations is that which precedes any instability. For the configurations with suction, the critical mass flow and the peak pressure recovery decreased almost linearly with increase in S/R . At S/R of 0.169, the peak recovery was decreased about 2.5 percent below the value for S/R of 0.

The performance summary of the inlet with cowl perforations (fig. 7(c)) indicates that the maximum stable subcritical operation was obtained with two rows of cowl perforations. Compared with the unmodified-cone performance, the stable subcritical range was increased by about 11 percent of the free-stream mass flow at zero angle of attack. At an angle of attack of 3° this increase was 6 percent while at an angle of attack of 6° the stable range was about the same as that for the unmodified cone. Subcritical recoveries, in some cases, were increased at zero angle of attack (fig. 5), possibly because of the removal of some of the higher-entropy flow resulting from the strong part of the terminal shock. At angle of attack, however, the perforations did not do this as effectively and probably not at all on the windward side of the cowl.

The critical inlet mass flow for the double row of cowl perforations was less than that for the single-row configurations at α of 0° (fig. 7(c)). This "critical" mass flow is defined as that which is measured at the diffuser exit when the terminal shock is at the inlet lip. For supercritical points with the shock downstream of the cowl lip, the higher mass flows with cowl perforations indicate that injection was occurring through the holes (fig. 5). This injection effect probably occurred for all shock positions on the windward side of the cowl at angle of attack (figs. 5 and 7(c)). At the critical shock position, the shock was upstream of the perforations. At this position the flow spillage through the holes was close to maximum since the static-pressure ratio

across the holes is only slightly different for subcritical conditions. From these considerations it is evident that any increase in stable subcritical range was not due to a loss of flow through the perforations. That is to say, the perforations did not simply serve as a bypass.

The performance summary of the configuration with cowl perforations combined with injection (fig. 7(d)) indicates that the maximum stable subcritical operation was achieved at S/R of 0.169 at zero angle of attack and 0.0565 at 3° and 6° angles of attack. In comparison with the unmodified-cone performance, the stable subcritical range was increased 21, 16.5, and 10.5 percent of the free-stream mass flow at angles of attack of 0° , 3° , and 6° , respectively. In comparison with the pure-injection case (fig. 7(a)), the use of injection plus cowl perforations showed no improvement though the values of S/R which gave maximum stability were changed. Also the peak pressure recoveries were about the same as the corresponding injection configurations.

Shadowgraphs of the supercritical and minimum stable mass-flow conditions are presented in figures 8 to 11 for the various configurations. In figure 8 for the unmodified cone, minimum stable operation occurred when the vortex sheet entered the inlet at 0° and 3° angles of attack. At a 6° angle of attack, the vortex sheet was outside of the inlet; however, there was extensive separation on the leeward spike surface at both 3° and 6° angles of attack. In figures 9 and 10 for the injection and suction cases, respectively, stable entrance of the vortex sheet was observed. Also, the amount of separation on the leeward cone surface was reduced by both modifications. With cowl perforations (fig. 11), stable entry of the vortex sheet was again made. Separation on the cone surface was not as extensive as for the unmodified-cone case, probably because the surface discontinuity of the bleed slot induced early transition to turbulent flow.

Secondary-Flow Requirements

The total pressures and mass flows through the secondary-flow passage are presented in figures 12 and 13 for the injection and suction cases, respectively. For injection the bleed mass-flow ratio was insensitive to angle of attack but increased as the spike gap was increased (fig. 12(a)). The maximum bleed flow was about 3 percent of the free-stream inlet mass flow. This increase in bleed mass flow with gap width partially accounted for the small supercritical inlet mass-flow variation with S/R for the injection case (fig. 3) as compared with the no-flow case (fig. 2).

The total pressure of the injected air decreased slightly as the spike gap width was increased (fig. 12(b)). This reduction was due to the added losses in the secondary-flow passage as the flow velocities increased. The average total pressure was about equal to the free-stream

total pressure. It was observed that any throttling of the secondary flow reduced the stable range for any value of S/R . (Similar effects are noted in ref. 7.) The inlet itself could not have been used as the supply of this high-pressure air since the pressure requirements are too high. Either an auxiliary pump or a compressor bleed supply are conceivable sources of injection air in an actual installation.

The secondary mass flow with cone suction (fig. 13(a)) was about 1 percent of the free-stream capture mass flow for all gap widths and angles of attack. The critical inlet mass flows with suction (fig. 4) are less than the critical mass flow without suction (fig. 2) by approximately this bleed-flow value. Throttling the bleed flow to approximately one-half of its maximum value did not significantly affect the stable operating range.

The secondary total-pressure recovery with cone suction (fig. 13(b)) decreased as the gap width increased at zero angle of attack. At angle of attack this spread was reduced, and the maximum total pressure was about 20 percent of the free-stream total pressure. It should be noted that these pressures were computed using the measured mass flows, static pressures, and known area and were considerably less than the theoretical cone static pressure (i.e., $p/P_0 = 0.35$).

Comparison of Various Stabilizing Methods

The maximum stable mass-flow range for each configuration is shown in figure 14. At zero angle of attack the configurations using suction, injection, and injection plus cowl perforations had nearly the same stable range. However, over the angle-of-attack range investigated, the most stable configuration was that achieved by the use of suction on the cone surface. As mentioned previously, for some configurations the minimum stable point presented was a prelude to a range of small amplitude instability with subsequent stabilization on the slot lip (fig. 4). Therefore, for these configurations the stable range might be considered larger than the stated values.

It might be questioned whether or not gains in stability could have been obtained by mixing the boundary layer on the cone. In an attempt to answer this question, the inlet of reference 5 was tested with and without tip roughness and a wire boundary-layer trip. The trip was located at approximately one-half the cone tip slant height. The minimum stable and critical mass-flow ratios for these configurations are presented in figure 15. It should be noted that this unmodified-cone data are not those of reference 5 but the result of a retest. There are small differences in results (fig. 2) though these are within experimental accuracy. Gains in stability are evident for all angles of attack with roughness, but the maximum gain is only 3 percent of the free-stream mass flow. The

gain in stability was slightly greater in the case of the wire trip at zero angle of attack (6 percent of free-stream mass flow); however, the stable range decreased for increasing angle of attack. In fact, a loss of 2 percent was observed at an angle of attack of 6° . In any case, the gains produced by mixing the boundary layer by these methods were not very large.

Shadowgraphs of the minimum stable configurations for 0° , 3° , and 6° angles of attack, for the cases of the wire trip and tip roughness, are presented in figure 16. The supercritical configurations were, as far as spillage was concerned, identical with the corresponding cases of the unmodified cone (fig. 8). It is important to note that, for both the wire trip and tip roughness at zero angle of attack (fig. 16(a)), the vortex sheet is inside the cowl. The cases of 3° and 6° angles of attack (figs. 16(b) and (c), respectively) are similar to that of the unmodified cone.

Effect of Stabilizing Devices on Flow Distortion

The distortion of the total-pressure profiles at the diffuser exit for the various secondary-flow devices is presented as a function of S/R in figure 17 for critical inlet operation. Distortion, in general, decreased as the spike gap was increased. Also, the least distortion was generally attained with no secondary flow. In any case the differences were not large. Some diffuser total-pressure contour maps of pressures measured at the diffuser rake are presented in figure 18.

SUMMARY OF RESULTS

An investigation was made, at Mach 1.91, of the stability characteristics of an axisymmetric conical inlet with supercritical spillage. This configuration had been previously reported to become unstable upon entry of the vortex sheet. The inlet incorporated modifications of a rearward-facing bleed slot on the external cone surface and/or cowl perforations. Injection or suction could be applied through the slot. The principal results of this investigation may be summarily described as follows:

1. Energizing the boundary layer by injecting air on the external-compression surface increased the stable subcritical range over that of the unmodified cone as much as $23\frac{1}{2}$ percent of the free-stream mass flow.

2. Suction on the external-compression surface using a rearward-facing slot increased the stable subcritical range over that of the unmodified cone as much as 22 percent of the free-stream mass flow with only 1-percent bleed mass flow.

3. Cowl perforations improved the stable subcritical range as much as 11 percent of the free-stream mass flow over that of the unmodified cone and for some configurations produced a higher peak recovery.

4. There was no substantial difference between the performance of the injection configuration coupled with cowl perforations and that with injection alone.

5. Small increases in the stable subcritical range were obtained by modifying the inlet by the use of tip roughness or a wire boundary-layer trip. However, the increases were at most 6 percent of free-stream mass flow, compared with the unmodified cone, and in most cases less than this value.

6. Stable entrance of the vortex sheet was obtained with all tested inlet modifications.

7. Only small decreases in pressure recovery were associated with the increases in stability for all tested inlet modifications.

8. The configuration employing cone surface suction was the best of the tested stability devices at angle of attack.

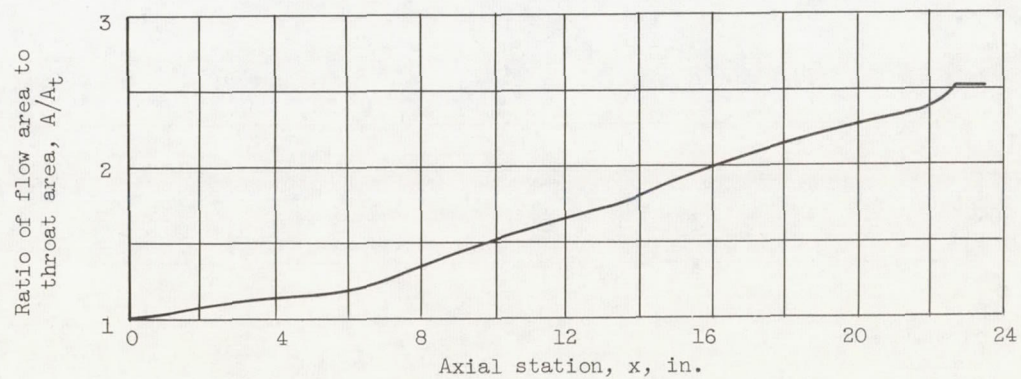
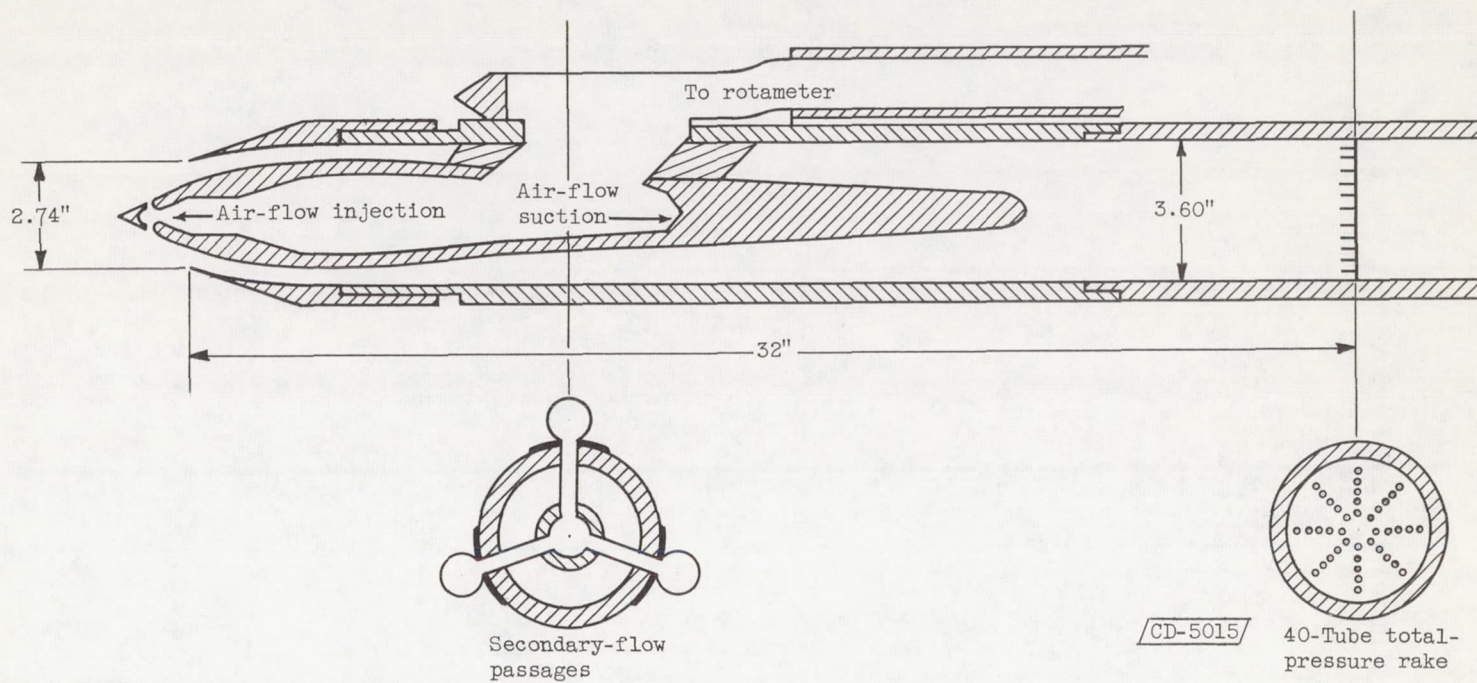
It is evident from the preceding results that entrance of the vortex sheet need not produce inlet instability if suitable boundary-layer control on the centerbody is provided.

Lewis Flight Propulsion Laboratory
National Advisory Committee for Aeronautics
Cleveland, Ohio, April 17, 1956

REFERENCES

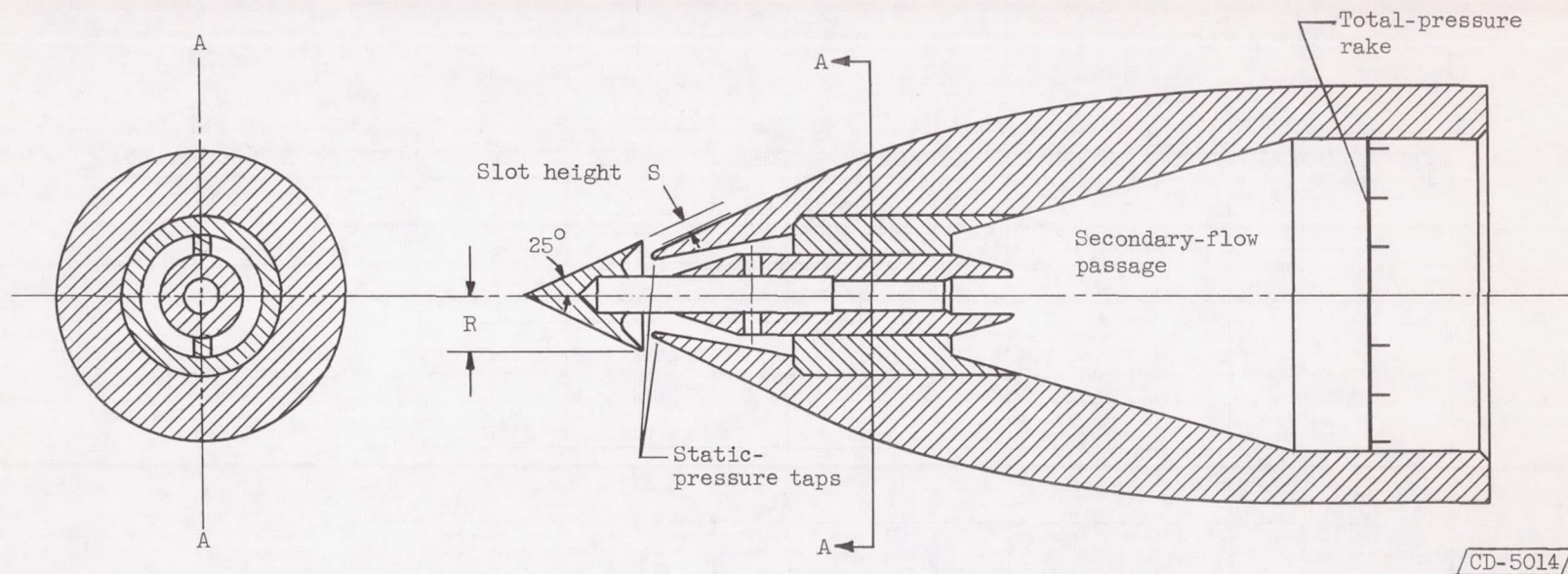
1. Dailey, Charles Lee: Supersonic Diffuser Instability. Jour. Aero. Sci., vol. 22, no. 11, Nov. 1955, pp. 733-749.
2. Ferri, Antonio, and Nucci, Louis M.: The Origin of Aerodynamics Instability of Supersonic Inlets at Subcritical Conditions. NACA RM L50K30, 1951.
3. Trimpi, Robert L., and Cohen, Nathaniel B.: Effect of Several Modifications to Center Body and Cowling on Subcritical Performance of a Supersonic Inlet at Mach Number 2.02. NACA RM L55C16, 1955.
4. Nussdorfer, T. J.: Some Observations of Shock-Induced Turbulent Separation on Supersonic Diffusers. NACA RM E51L26, 1954.

5. Beheim, Milton A.: A Preliminary Investigation at Mach 1.91 of a Diffuser Employing a Pivoted Cone to Improve Operation at Angle of Attack. NACA RM E53I30, 1953.
6. Conners, James F., and Meyer, Rudolph C.: Performance Characteristics of Axisymmetric Two-Cone and Isentropic Nose Inlets at Mach Number 1.90. NACA RM E55F29, 1955.
7. Piercy, Thomas G.: Preliminary Investigation of Some Internal Boundary-Layer-Control Systems on a Side Inlet at Mach Number 2.96. NACA RM E54K01, 1955.



(a) Area variation and instrumentation.

Figure 1. - Model geometry and instrumentation.



(b) Spike detail.

Figure 1. - Concluded. Model geometry and instrumentation.

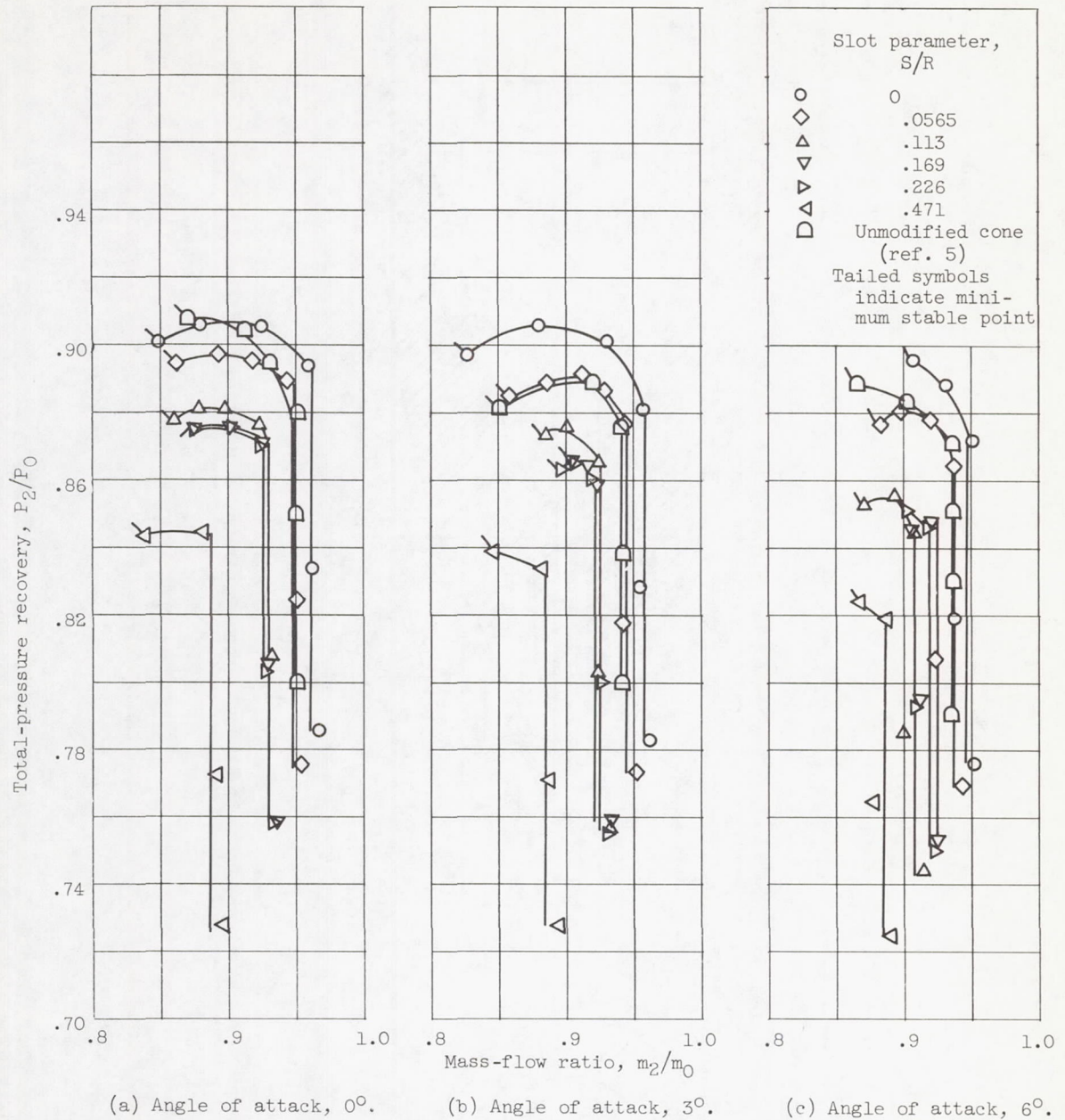


Figure 2. - Total-pressure - mass-flow characteristics for various slot sizes. No secondary flow.

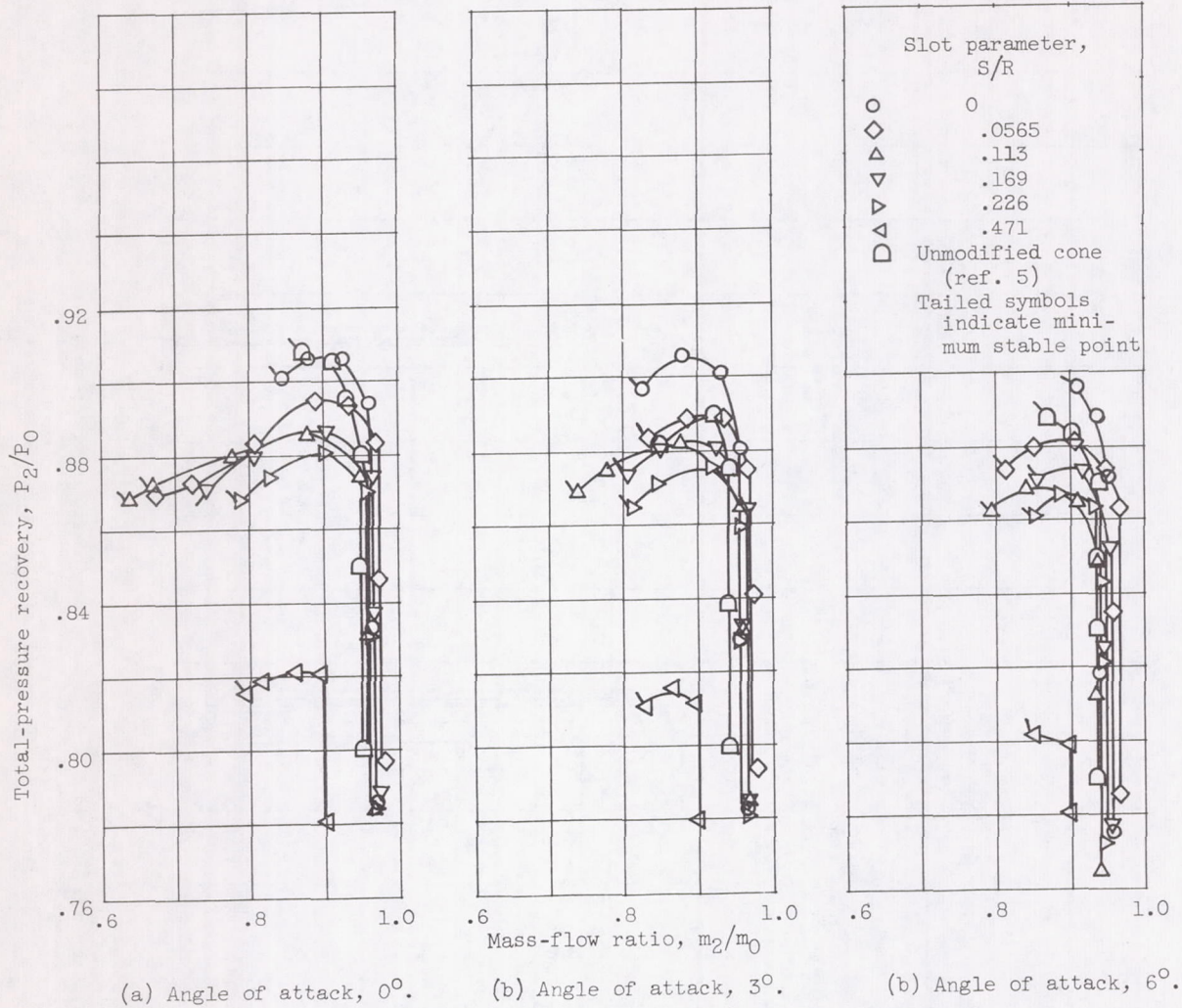


Figure 3. - Effect of injection on inlet performance.

3950

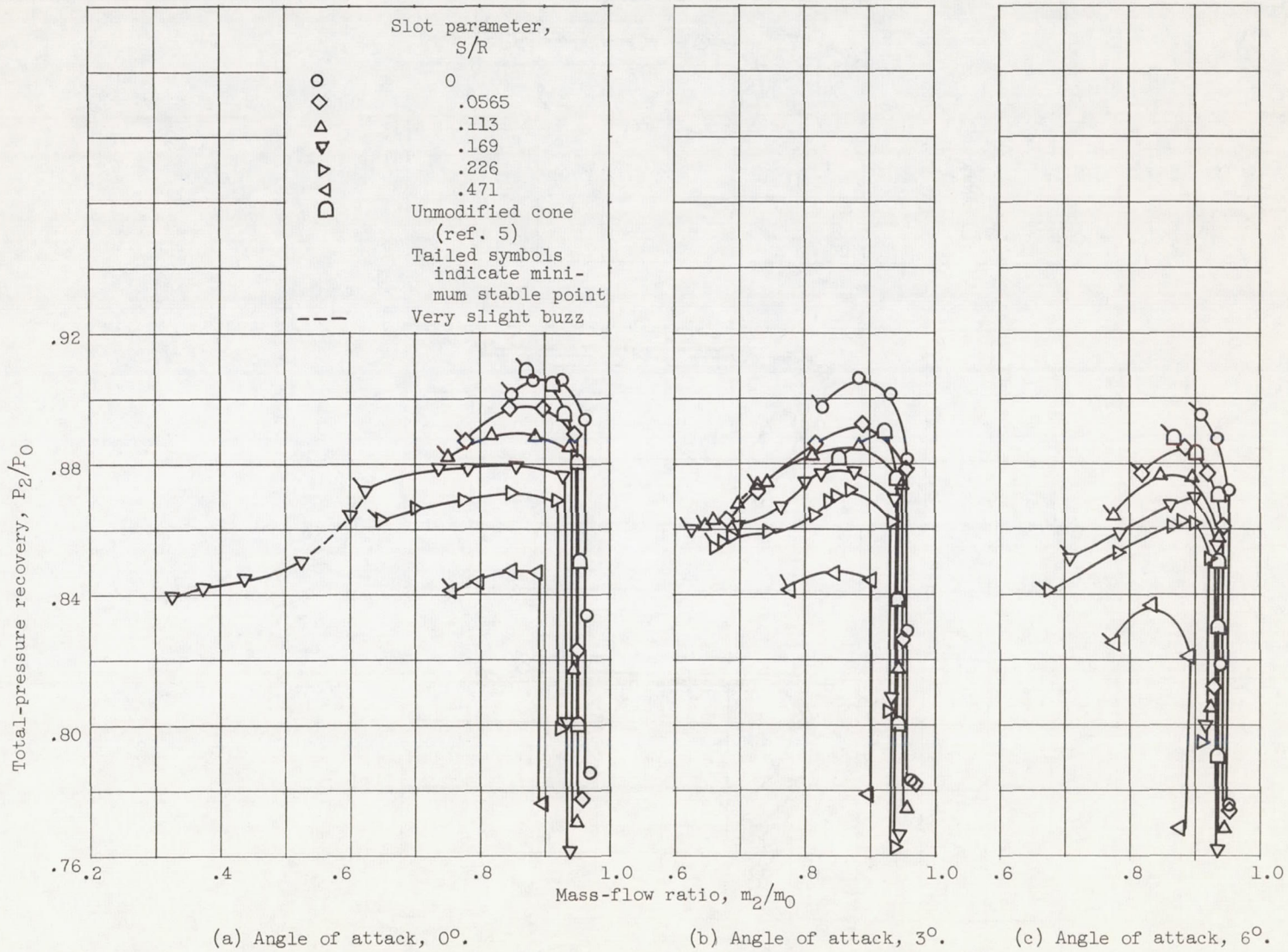


Figure 4. - Effect of suction on inlet performance.

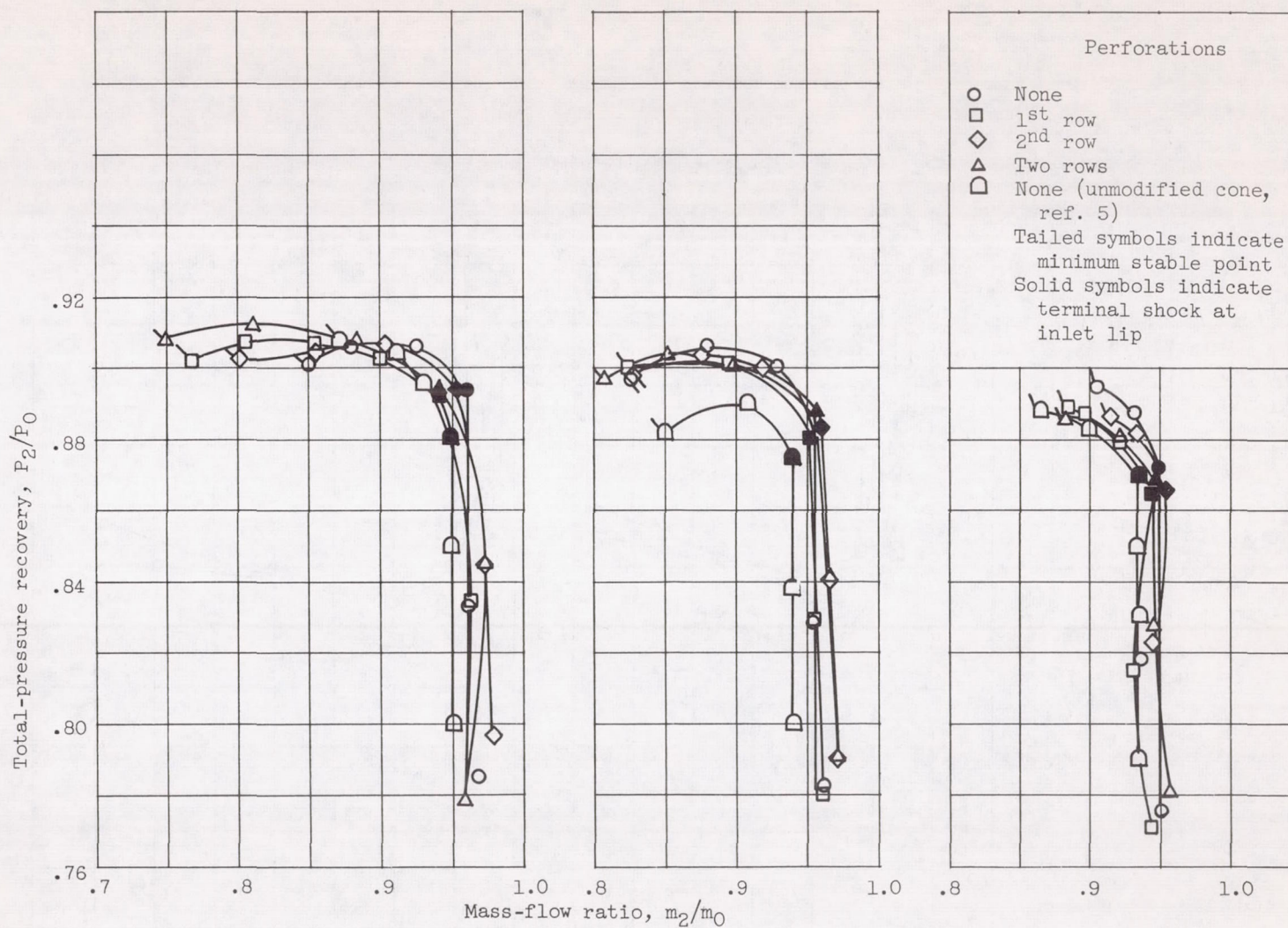


Figure 5. - Effect of cowl perforations on inlet performance.

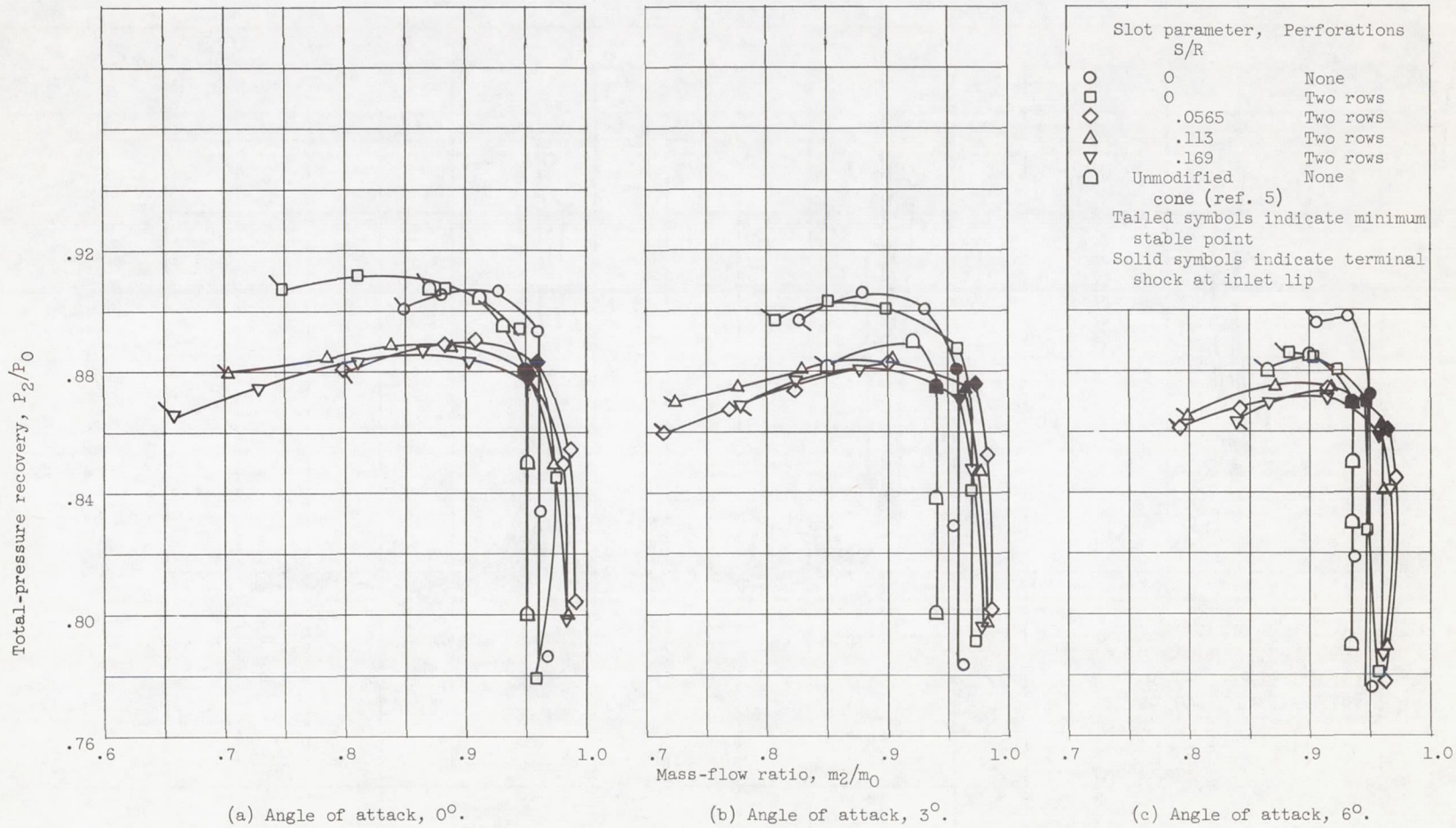
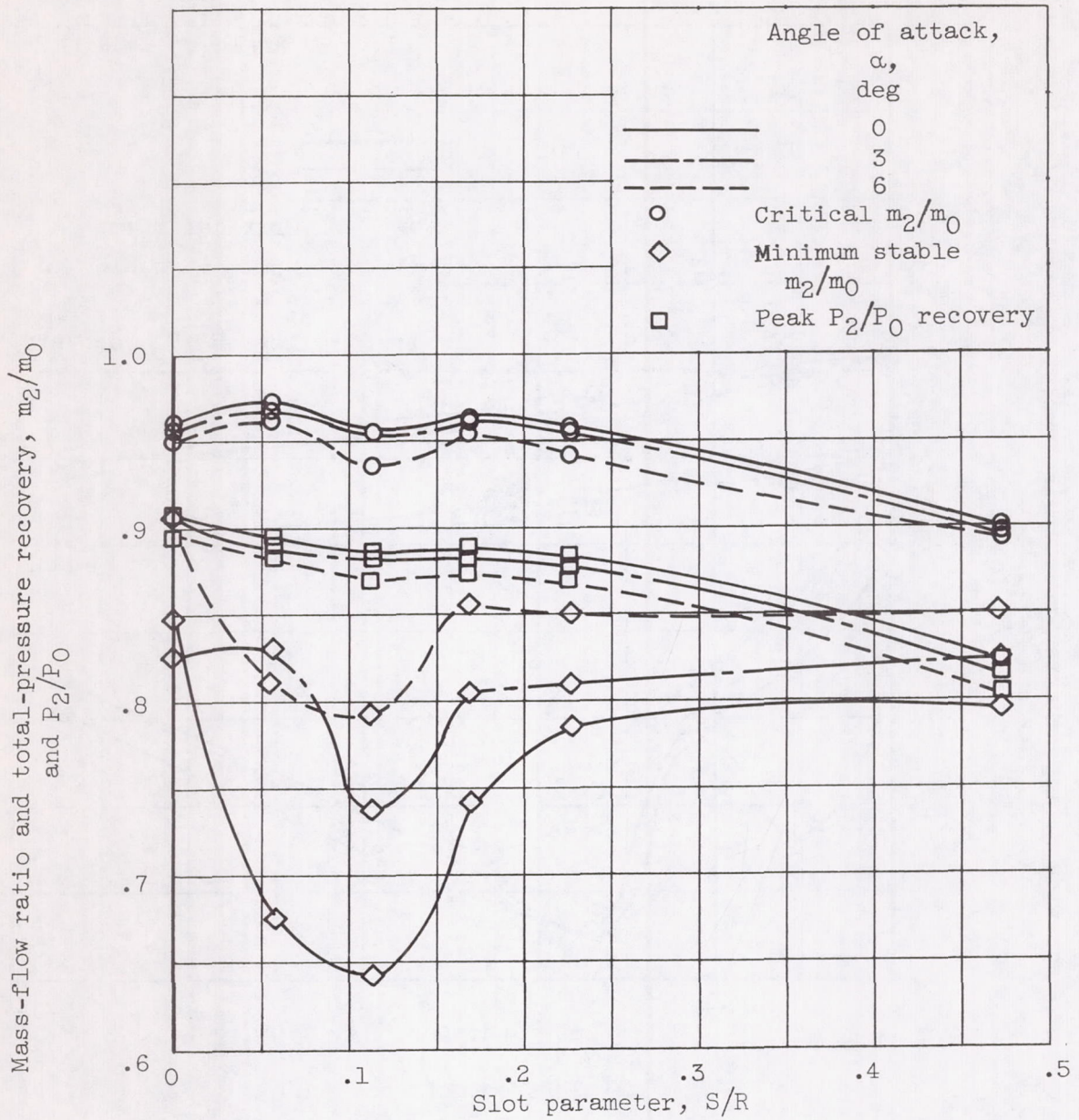
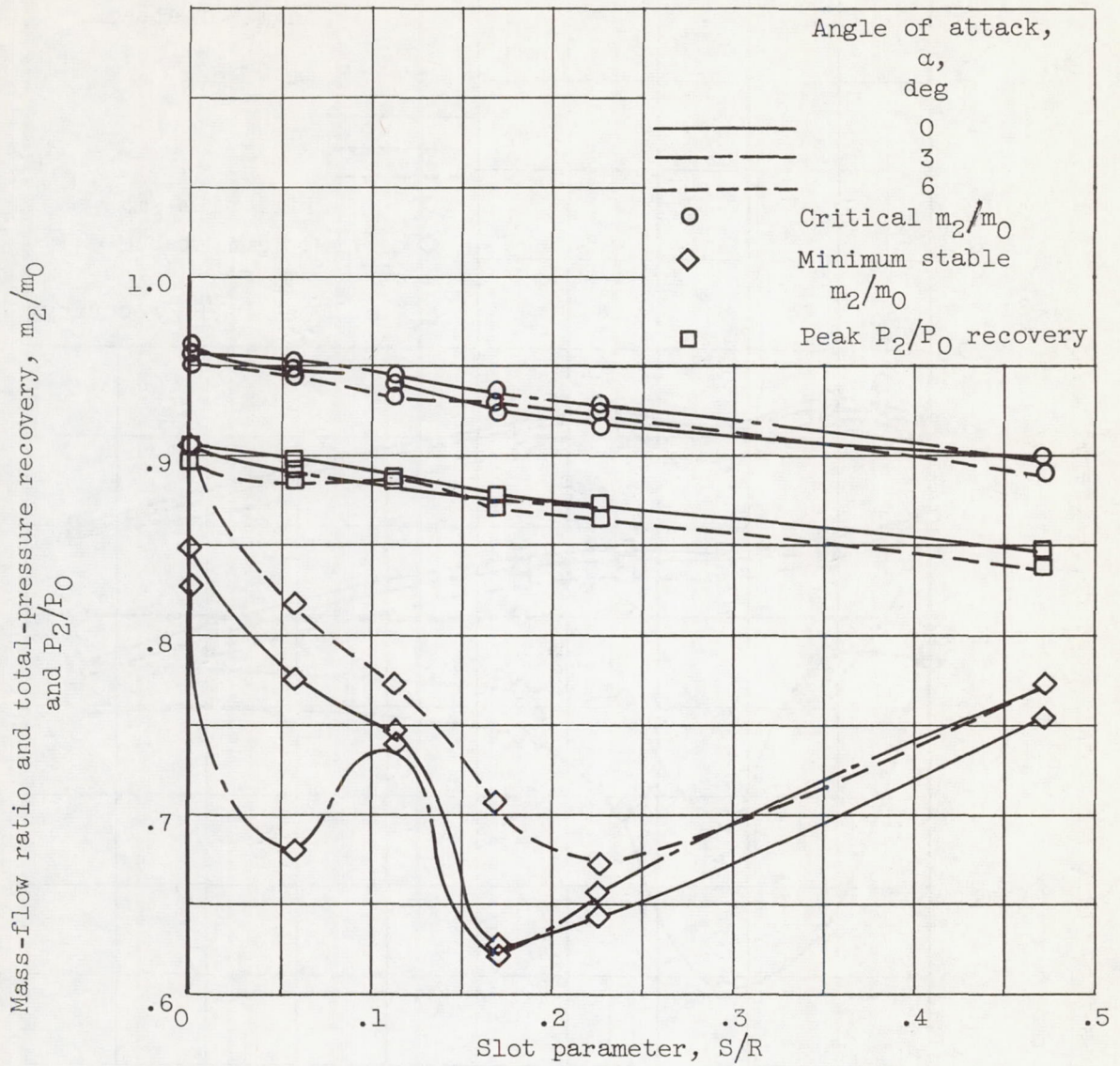


Figure 6. - Effect of injection plus cowl perforations on inlet performance.



(a) Effect of injection.

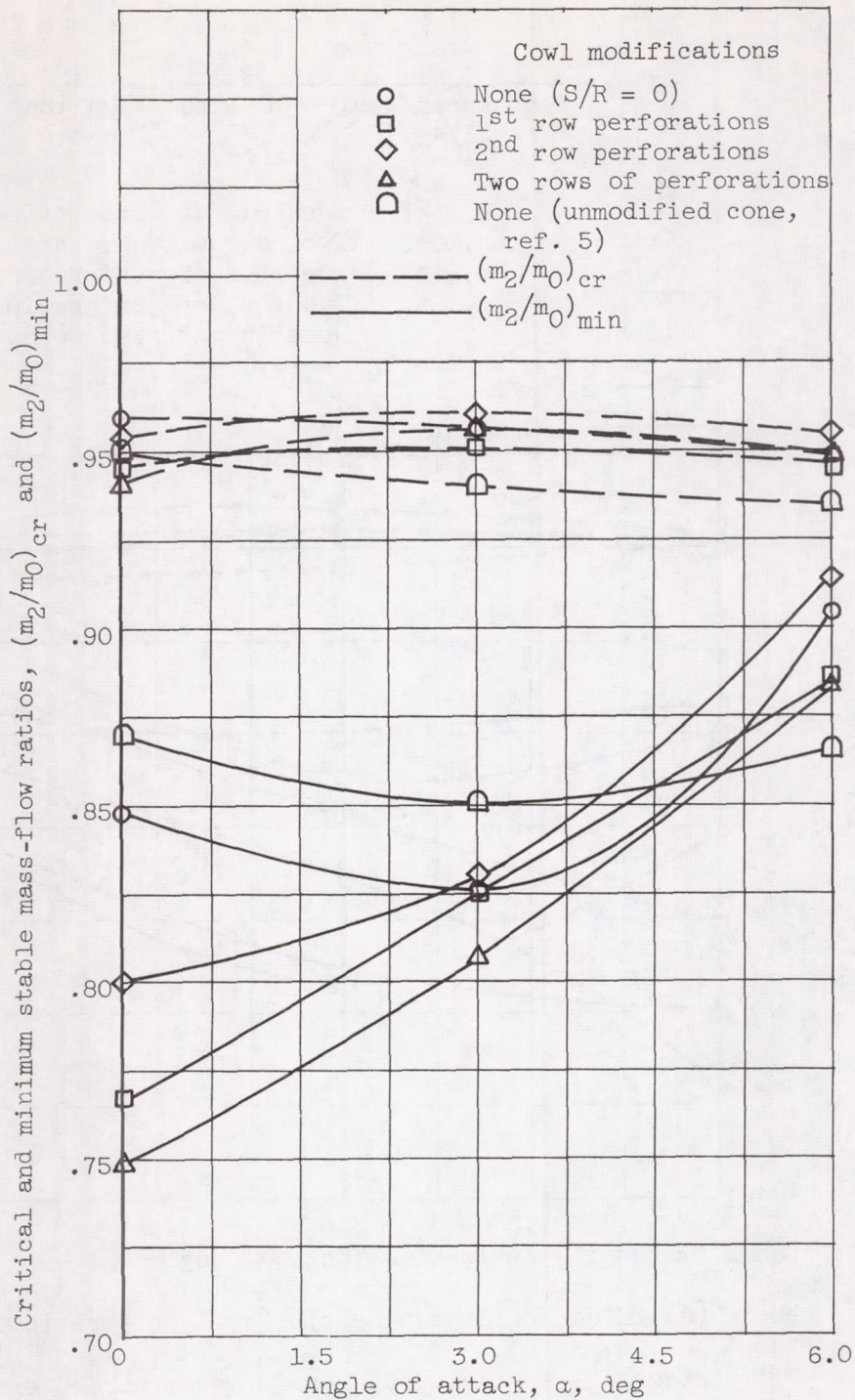
Figure 7. - Performance parameters.



(b) Effect of suction.

Figure 7. - Continued. Performance parameters.

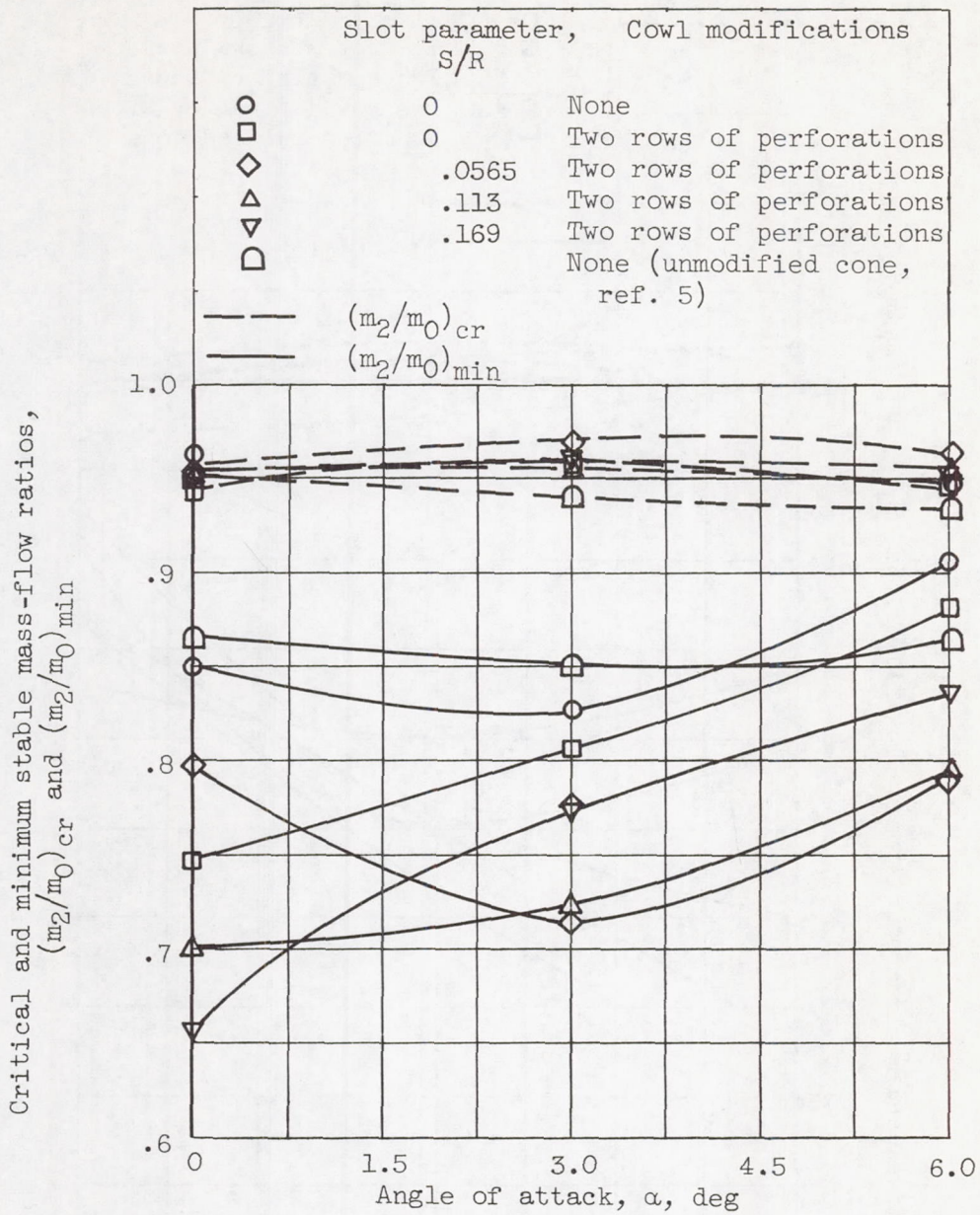
3950



(c) Effect of cowl perforations.

Figure 7. - Continued. Performance parameters.

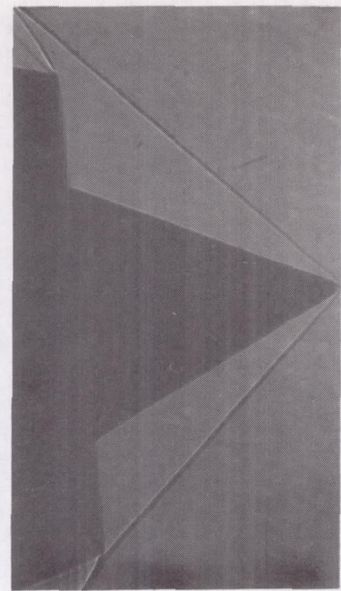
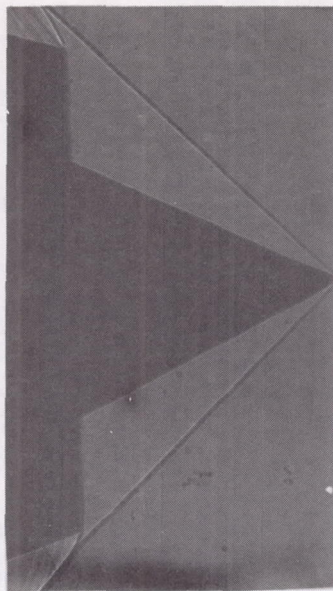
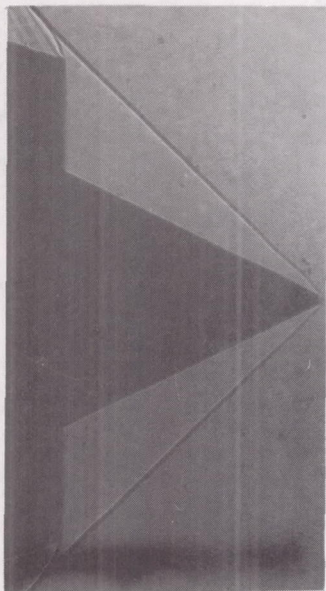
3950



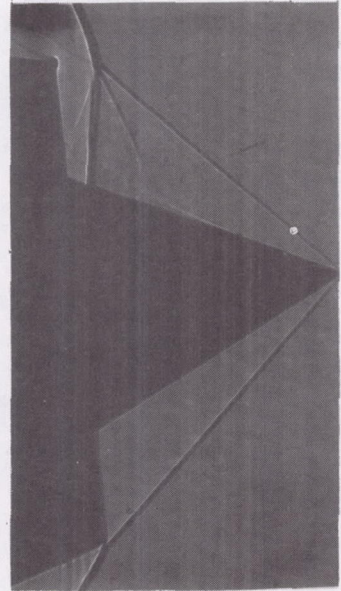
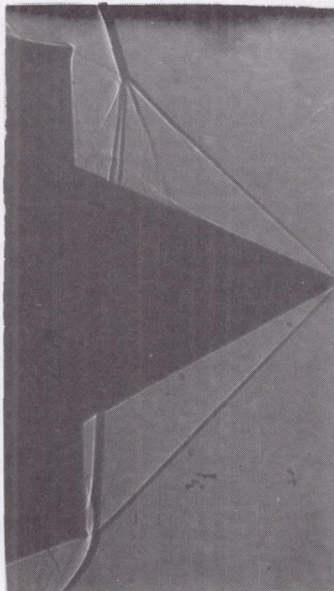
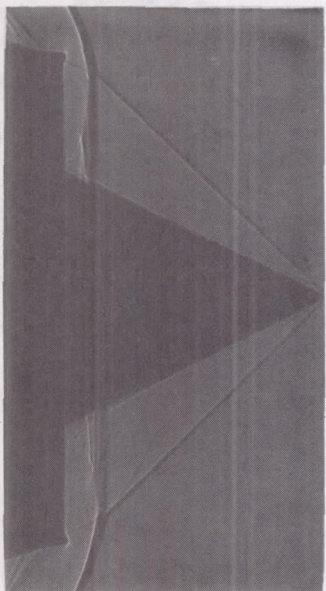
(d) Effect of injection plus cowl perforations.

Figure 7. - Concluded. Performance parameters.

3950



Supercritical mass flow



Minimum stable mass flow

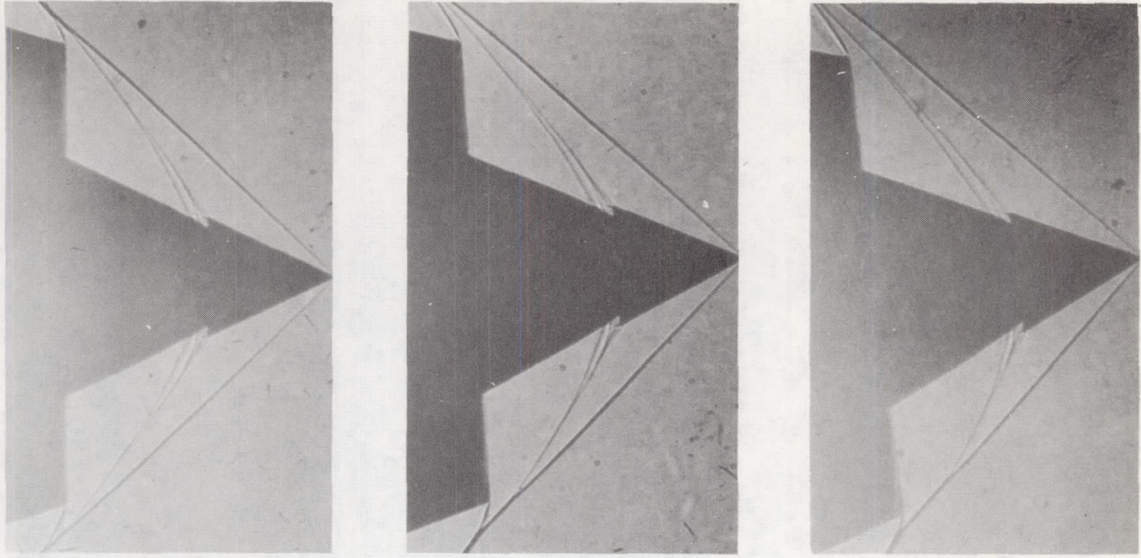
C-41706

(a) Angle of attack, 0° .

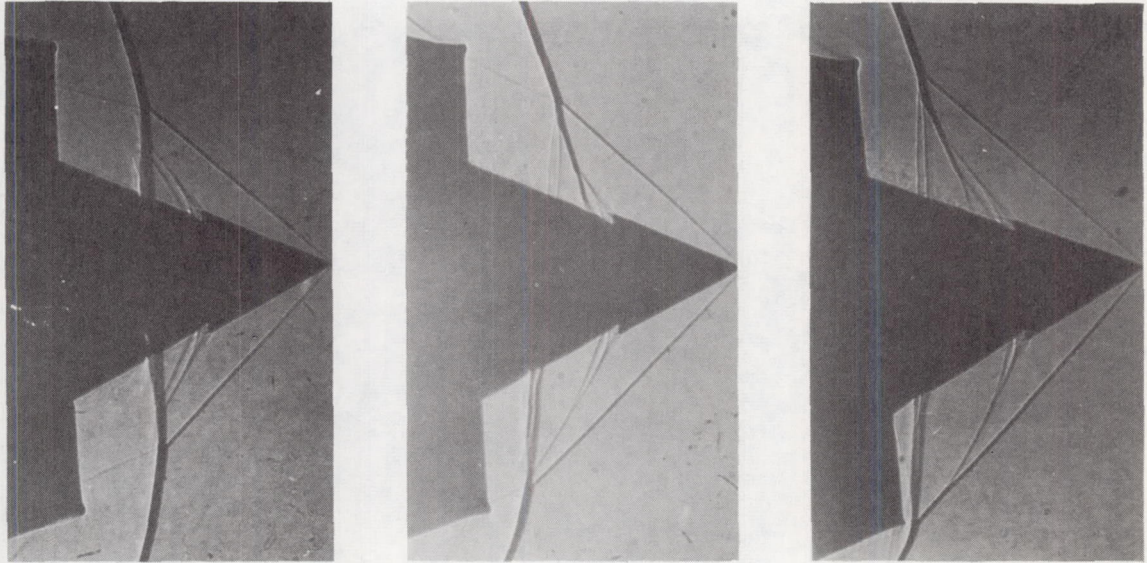
(b) Angle of attack, 3° .

(c) Angle of attack, 6° .

Figure 8. - Supercritical and minimum stable mass-flow configurations for unmodified cone.



Supercritical mass flow



Minimum stable mass flow

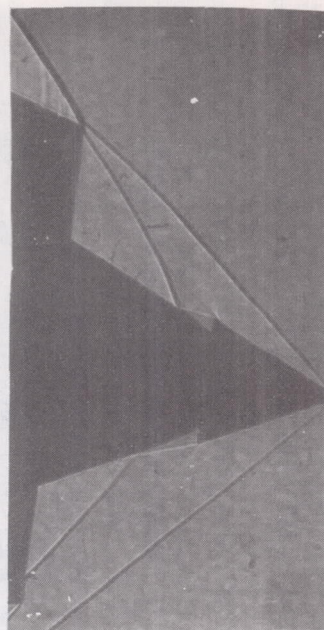
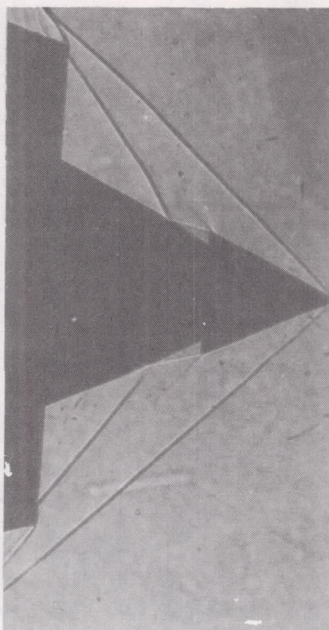
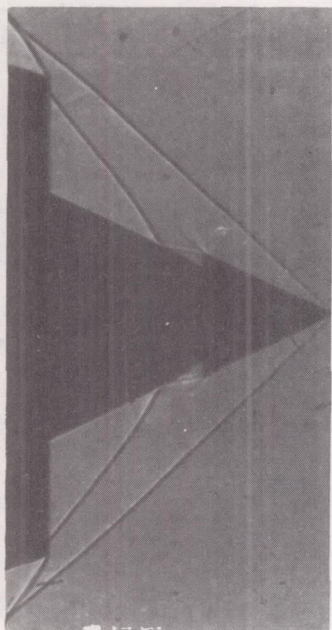
C-41707

(a) Angle of attack, 0° .

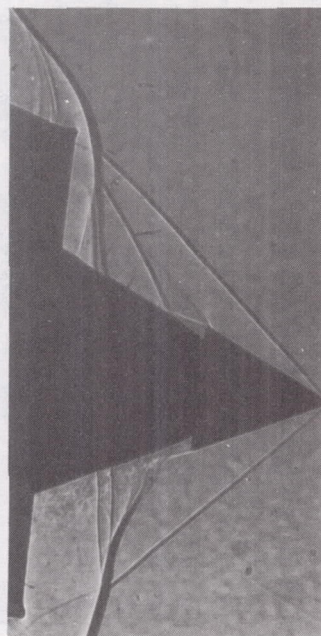
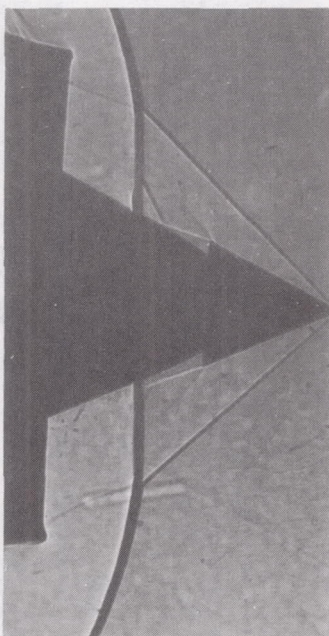
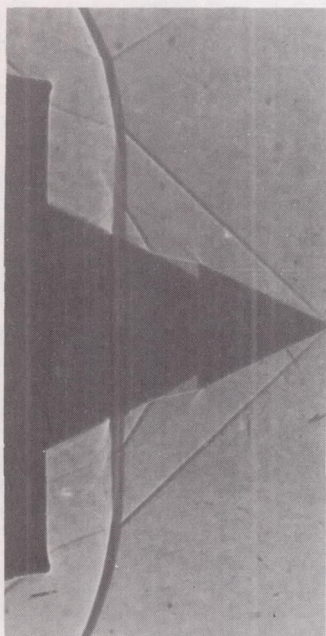
(b) Angle of attack, 3° .

(c) Angle of attack, 6° .

Figure 9. - Supercritical and minimum stable mass-flow configurations for s/R of 0.113 with injection.



Supercritical mass flow



Minimum stable mass flow

C-41708

(a) Angle of attack, 0° .

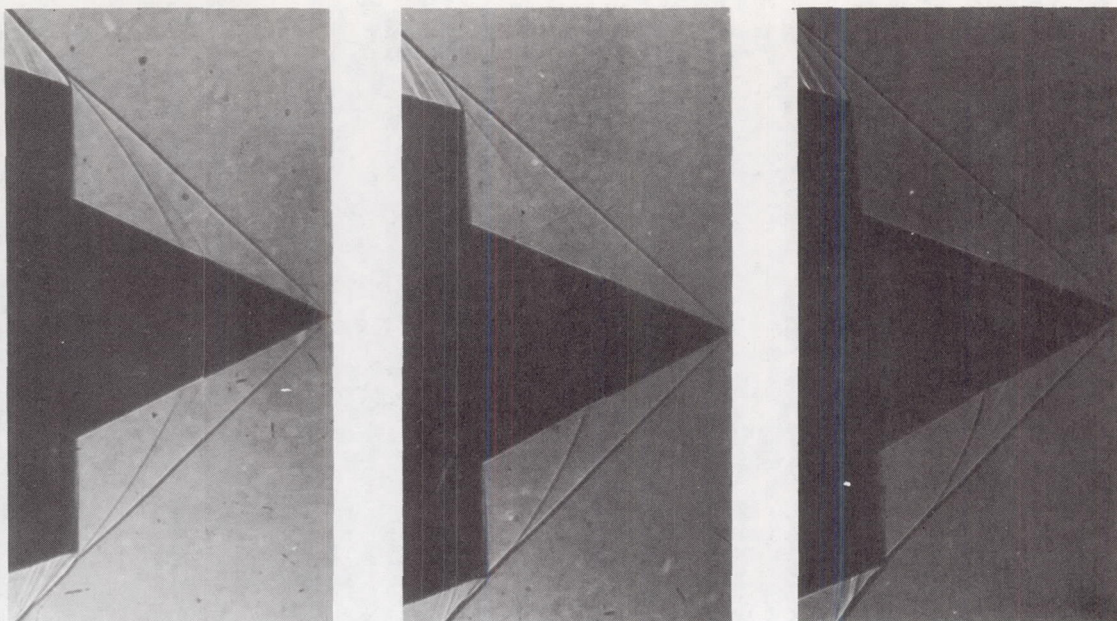
(b) Angle of attack, 3° .

(c) Angle of attack, 6° .

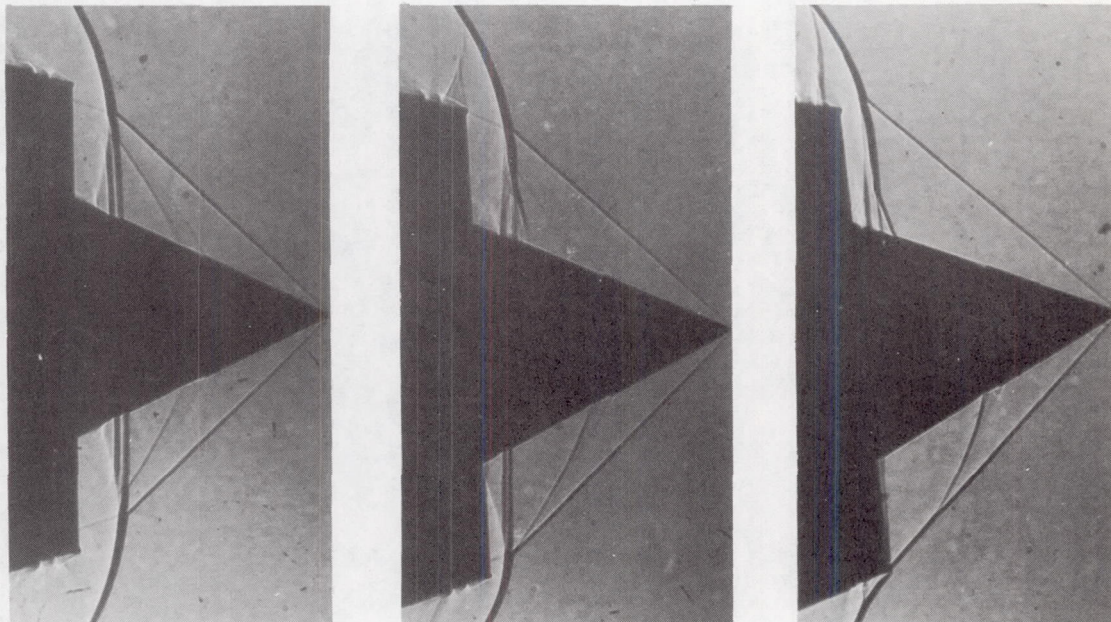
Figure 10. - Supercritical and minimum stable mass-flow configurations for s/R of 0.169 with suction.

3950

CP-4



Supercritical mass flow

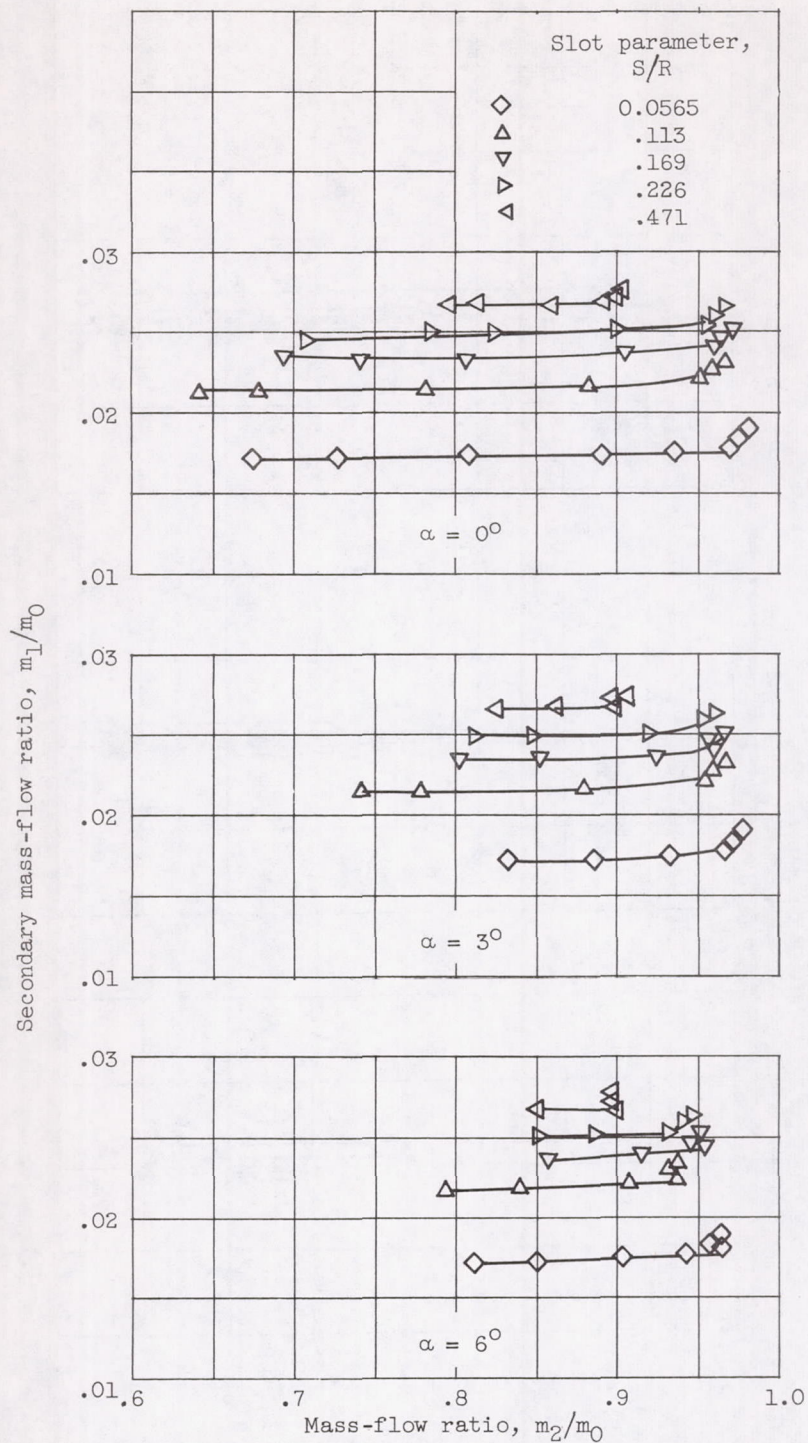


Minimum stable mass flow

C-41709

(a) Angle of
attack, 0° .(b) Angle of
attack, 3° .(c) Angle of
attack, 6° .

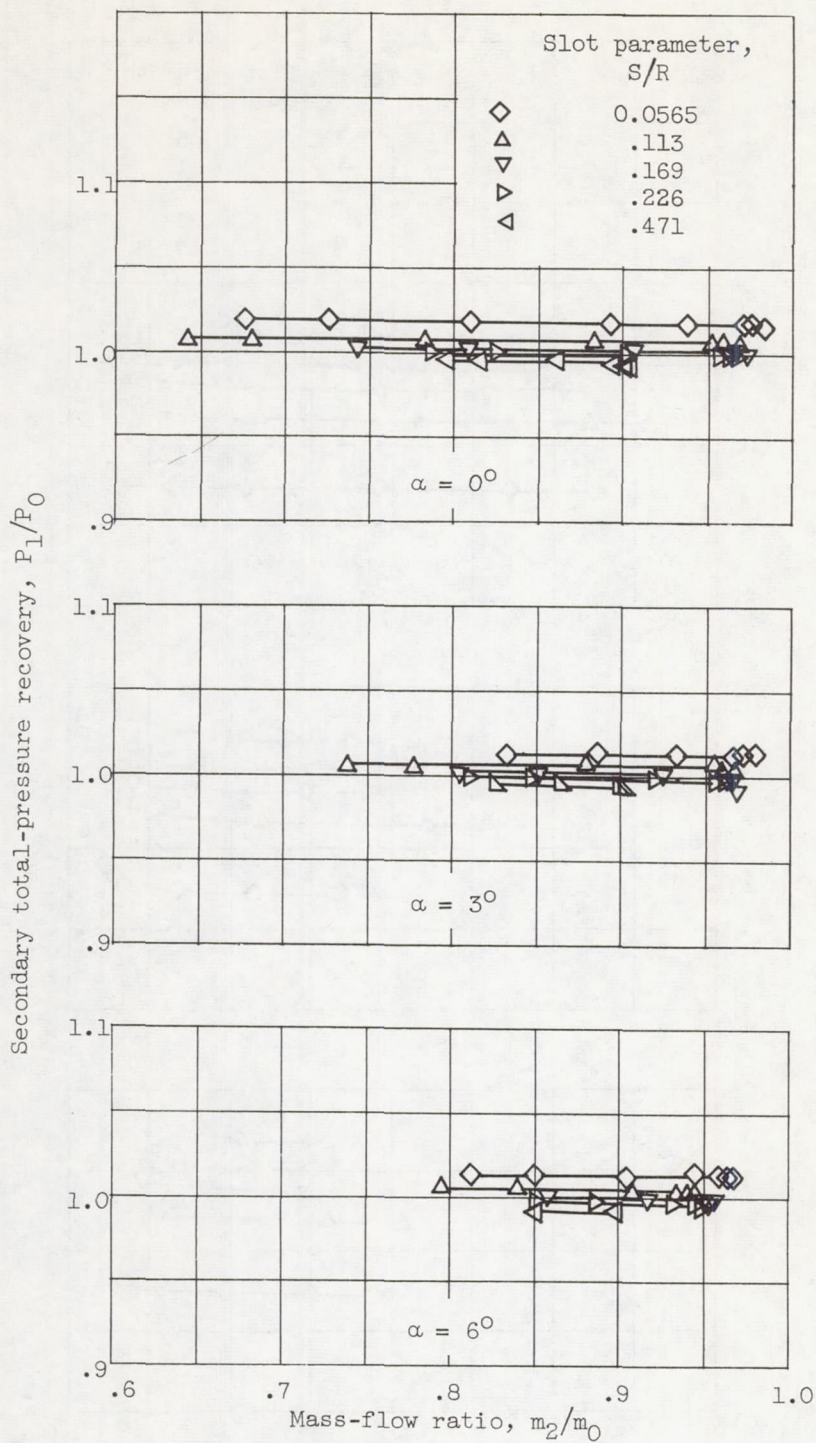
Figure 11. - Supercritical and minimum stable mass-flow configurations for s/R of 0 with two rows of cowl perforations.



(a) Mass flow.

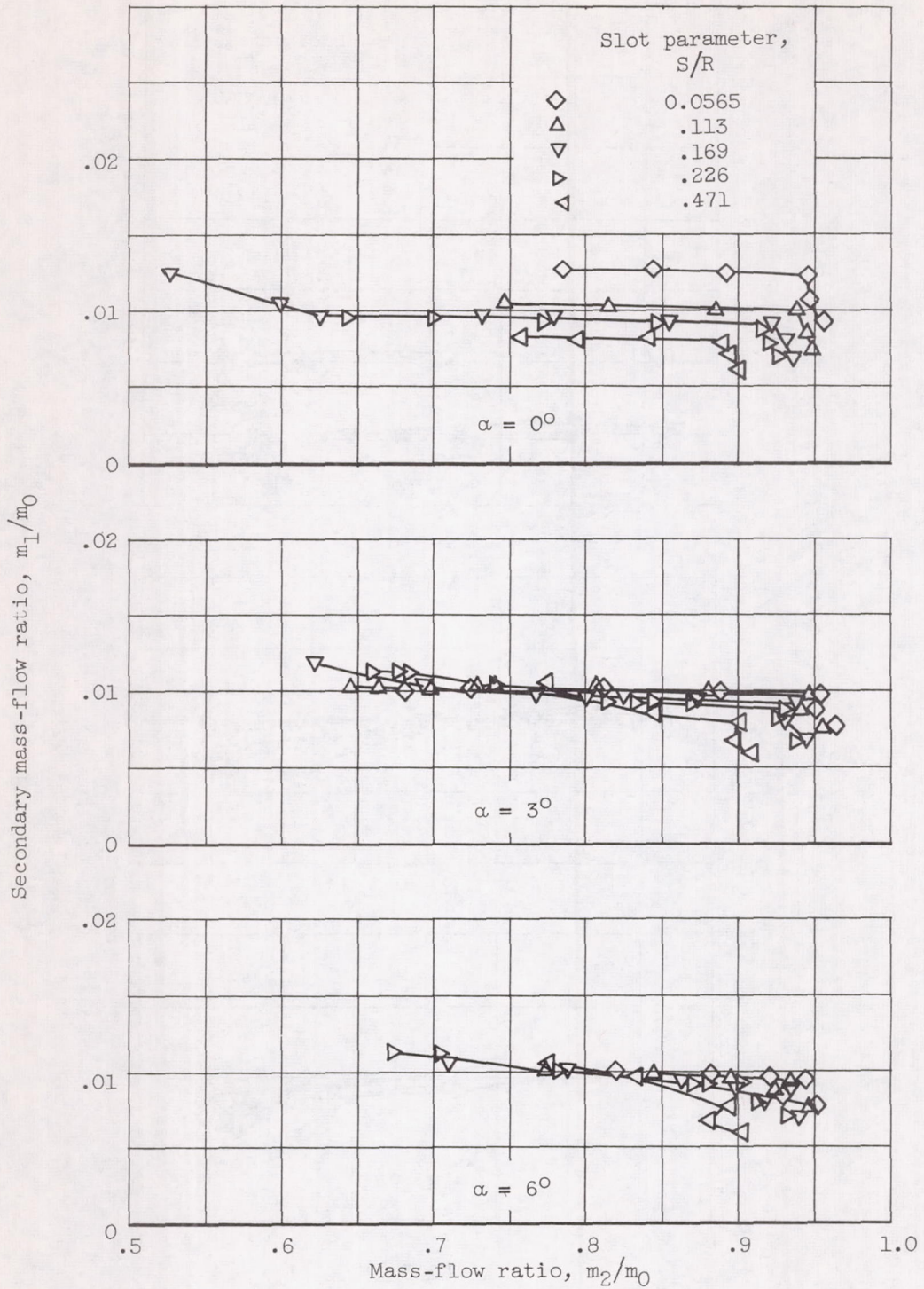
Figure 12. - Secondary-flow characteristics with injection.

CP-4 back, 3950



(b) Total pressure.

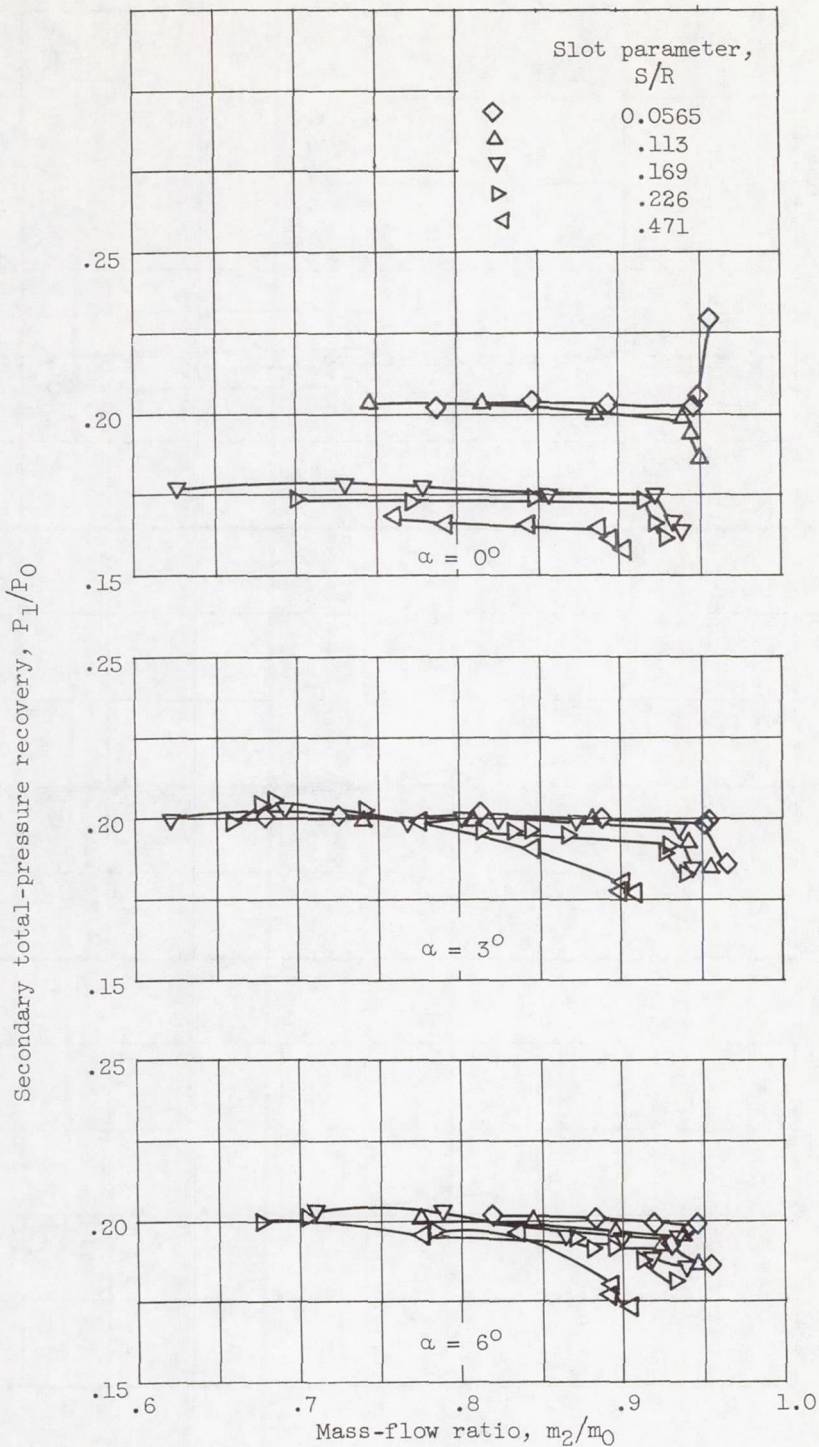
Figure 12. - Concluded. Secondary-flow characteristics with injection.



(a) Mass flow.

Figure 13. - Secondary-flow characteristics with suction.

3950



(b) Total pressure.

Figure 13. - Concluded. Secondary-flow characteristics with suction.

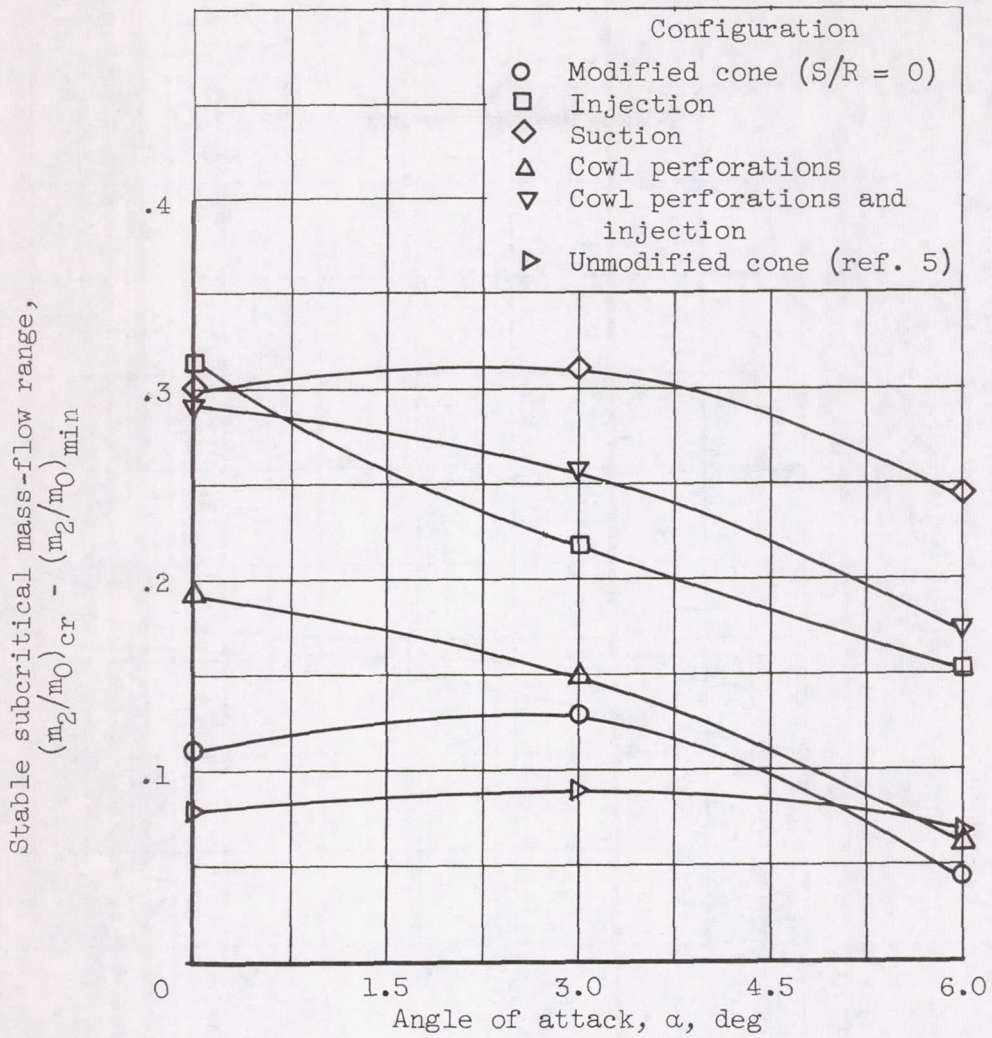


Figure 14. - Comparison of maximum stable mass-flow range for each configuration.

3950

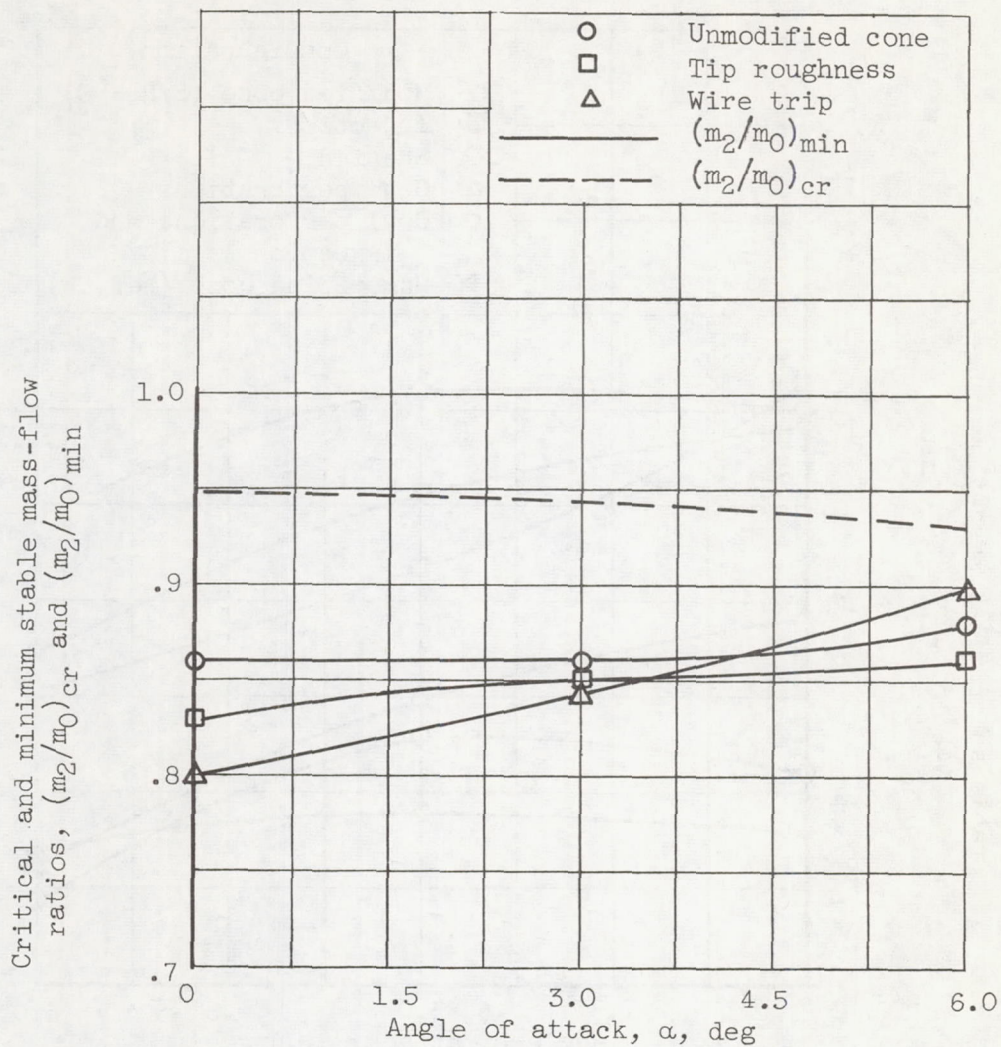
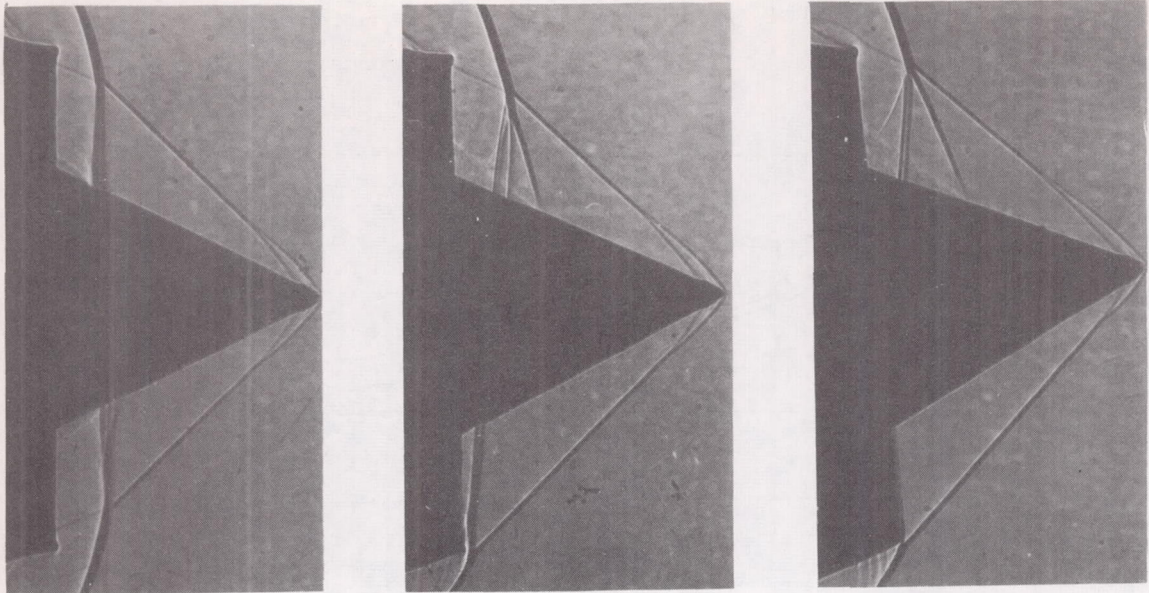
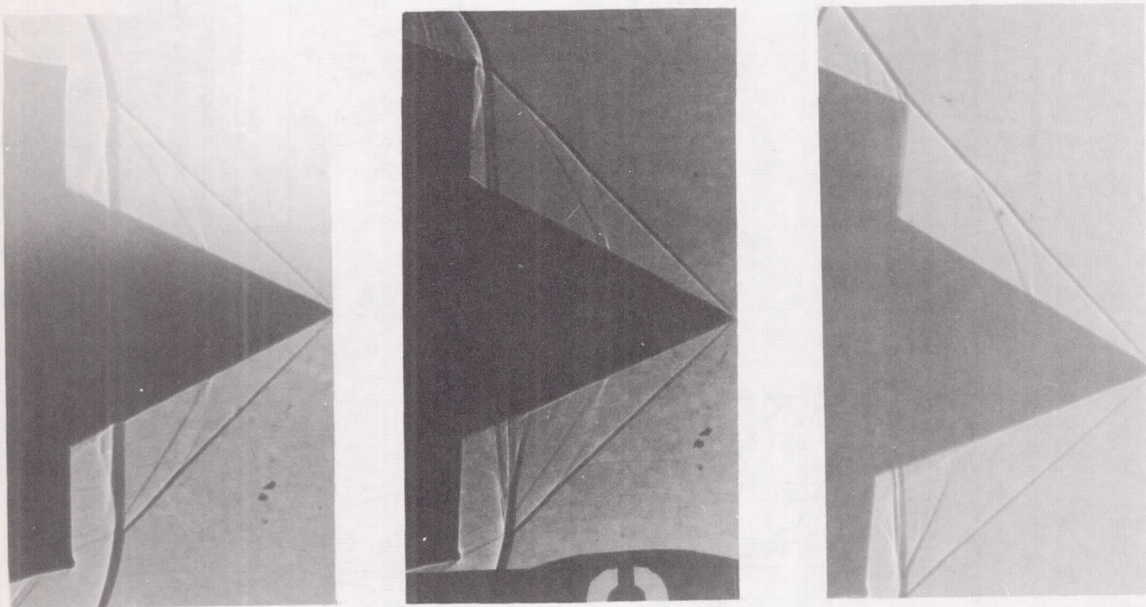


Figure 15. - Effect of tip roughness and wire trip on stability.



Tip roughness



Wire trip.

C-41710

(a) Angle of attack, 0° .

(b) Angle of attack, 3° .

(c) Angle of attack, 6° .

Figure 16. - Minimum stable mass-flow configurations for unmodified cone with tip roughness and with wire trip.

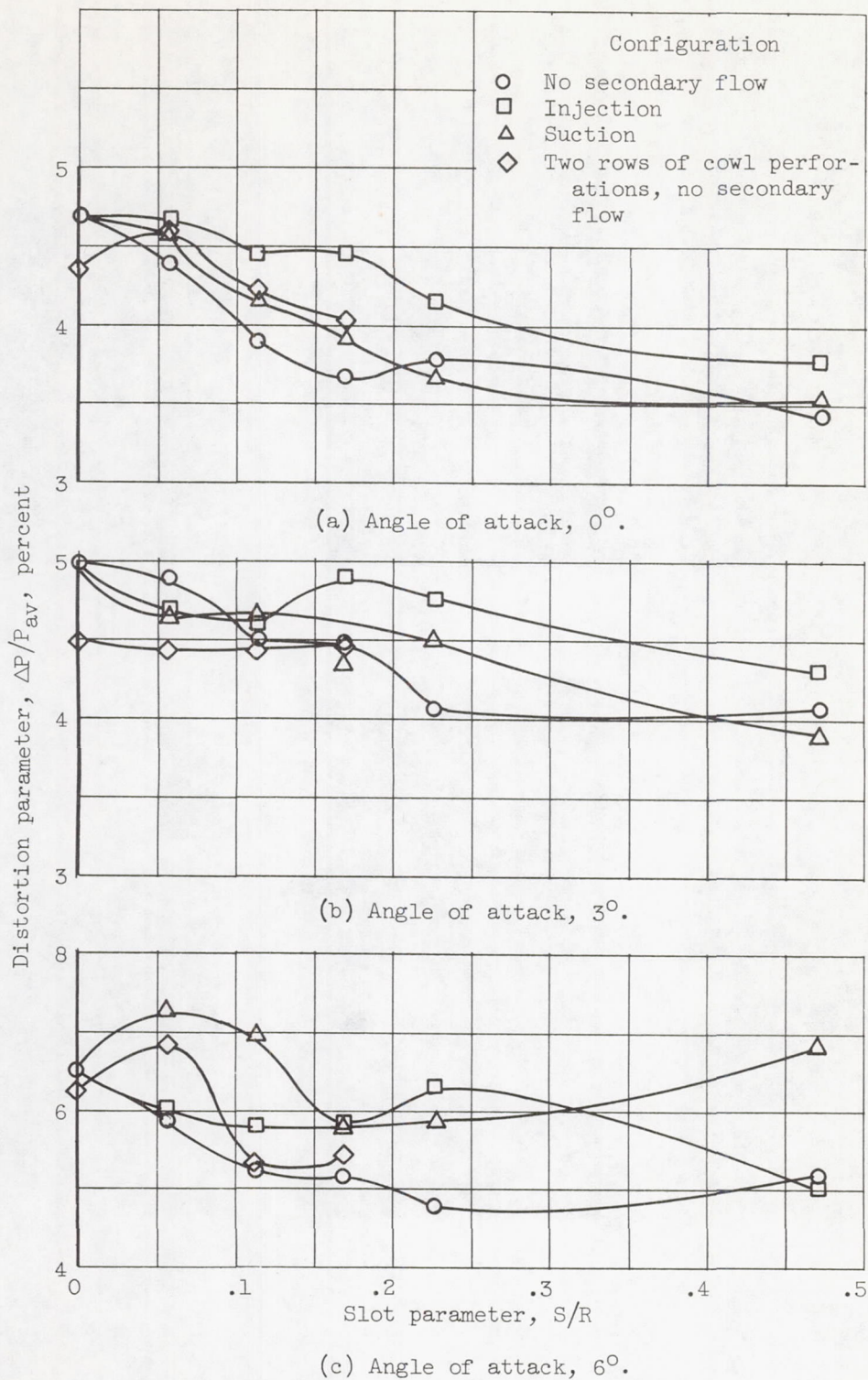
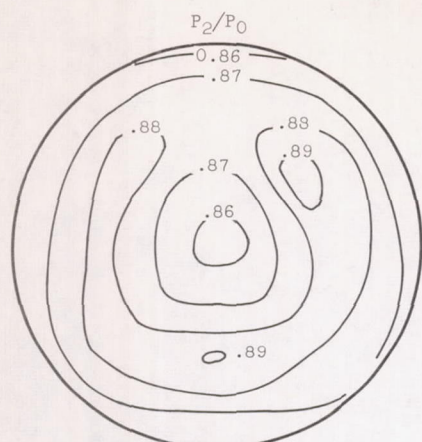
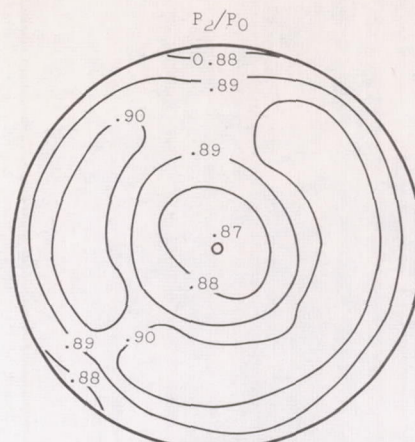


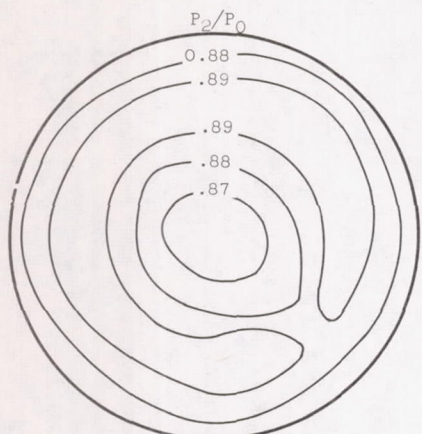
Figure 17. - Distortion as function of slot size for various configurations.



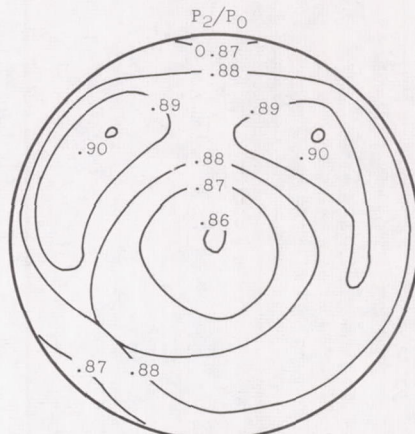
(a) Slot parameter, 0.113; angle of attack, 0° ; critical pressure recovery; injection.



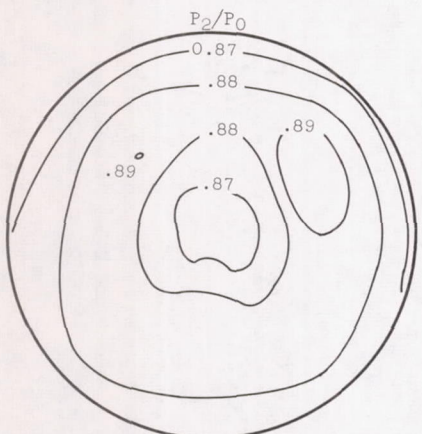
(b) Slot parameter, 0; angle of attack, 0° ; critical pressure recovery.



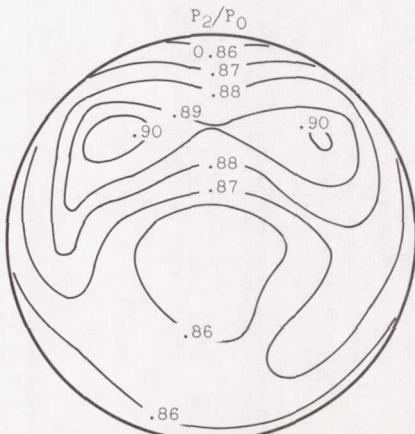
(c) Slot parameter, 0.113; angle of attack, 0° ; critical pressure recovery; suction.



(d) Slot parameter, 0; angle of attack, 3° ; critical pressure recovery.



(e) Slot parameter, 0.113; angle of attack, 0° ; critical pressure recovery; injection; two rows of perforations.



(f) Slot parameter, 0; angle of attack, 6° ; critical pressure recovery.

Figure 18. - Total-pressure contour maps at station 2 of subsonic diffuser.

